Cross-Talk of Cells in the Heart 2025: Novel Mechanisms of Disease and Arrhythmias
University of Birmingham, UK | 03 – 04 September 2025

Experiments on animals and animal tissues

It is a requirement of The Society that all vertebrates (and Octopus vulgaris) used in experiments are humanely treated and, where relevant, humanely killed.

To this end authors must tick the appropriate box to confirm that:

For work conducted in the UK, all procedures accorded with current UK legislation.

For work conducted elsewhere, all procedures accorded with current national legislation/guidelines or, in their absence, with current local guidelines.

Experiments on humans or human tissue

Authors must tick the appropriate box to confirm that:

All procedures accorded with the ethical standards of the relevant national, institutional or other body responsible for human research and experimentation, and with the principles of the World Medical Association's Declaration of Helsinki.

Guidelines on the Submission and Presentation of Abstracts

Please note, to constitute an acceptable abstract, The Society requires the following ethical criteria to be met. To be acceptable for publication, experiments on living vertebrates and Octopus vulgaris must conform with the ethical requirements of The Society regarding relevant authorisation, as indicated in Step 2 of submission.

Abstracts of Communications or Demonstrations must state the type of animal used (common name or genus, including man. Where applicable, abstracts must specify the anaesthetics used, and their doses and route of administration, for all experimental procedures (including preparative surgery, e.g. ovariectomy, decerebration, etc.).

For experiments involving neuromuscular blockade, the abstract must give the type and dose, plus the methods used to monitor the adequacy of anaesthesia during blockade (or refer to a paper with these details). For the preparation of isolated tissues, including primary cultures and brain slices, the method of killing (e.g. terminal anaesthesia) is required only if scientifically relevant. In experiments where genes are expressed in Xenopus oocytes, full details of the oocyte collection are not necessary. All procedures on human subjects or human tissue must accord with the ethical requirements of The Society regarding relevant authorisation, as indicated in Step 2 of submission; authors must tick the appropriate box to indicate compliance.

Cross-Talk of Cells in the Heart 2025: Novel Mechanisms of Disease and Arrhythmias
University of Birmingham, UK | 03 – 04 September 2025

SA01

Cardiac fibroblast-myocyte crosstalk in hyperglycaemic and hypertensive conditions

Niall Macquaide[1], Zainab Olatunji[1], Susan Currie[2]

[1]Glasgow Caledonian University, United Kingdom, [2]University of Strathclyde, United Kingdom

Introduction

Heart Failure with preserved Ejection Fraction (HFpEF), is a multifactorial disease associated with hypertension, diabetes and obesity, and is predominantly observed in females1. HFpEF results in a slowly relaxing, fibrotic myocardium, and modifications in cardiomyocyte (CM) Ca^{2+}-handling-proteins are observed in animal models in vivo2. However, how patient comorbidities may influence cardiac fibroblasts (CFs) and how this may then influence myocytes in the HFpEF phenotype remains unclear. This study aims to develop an in vitro model -which includes aspects of HFpEF to explore abnormal Ca^{2+}-signalling of CFs and CMs in hyperglycaemic-hypertensive conditions.

Methods

Adult human male and female CFs (Promocell) and primary left ventricular CMs isolated from adult NZW male rabbits, were cultured independently or co-cultured using media containing 22mM Glucose (HG), 200nM Angiotensin-II (AngII) or a combination of both (to mimic diabetes, hypertension or HFpEF, respectively), for a duration of 24h. Both cell types were then loaded with 2μM Cal520AM calcium indicator. CFs were chemically stimulated using 20nM Endothelin-1 while CMs were electrically field-stimulated at 1Hz to generate Ca^{2+}-responses. The alterations in intracellular Ca^{2+} were measured by confocal microscopy.

Results

The Ca^{2+} transient amplitude (ΔF/F0) in CFs was enhanced with 22mM Glucose (HG) [Control: 0.158±0.015; HG: 0.273±0.014; n=3 humans with 3 technical replicates each; $p< 0.001$]. The Ca^{2+}-transient-amplitude in CMs increased with AngII [Control: 0.750±0.101; Hypertension: 2.02±0.32; N=3 rabbits; $p< 0.0001$]. In myocytes co-cultured with female CFs, the Ca^{2+}-transient-amplitude was sustained with HG and AngII [Control: 0.346±0.064; HG: 0.359±0.049; Ang: 0.296±0.037; N=3 rabbits]. However, Ca^{2+}-spark-frequency (sparks.μm^2.s^{-1}) in CMs was elevated after co-culture with female CFs, across all pathological conditions [Control: 3.56±0.71; Diabetes: 13.0±1.1; Hypertension: 16.5±1.1; HFpEF: 22.9±1.2; N=3 rabbits; $p< 0.001$].

Conclusions

These findings show remodelling of Ca^{2+}-signalling in CFs and CMs, in an in vitro model of HFpEF. A sex disparity observed in female co-culture mimics that seen in human HFpEF. Further work is needed to understand how this in vitro model correlates to an in vivo model of HFpEF.

Cross-Talk of Cells in the Heart 2025: Novel Mechanisms of Disease and Arrhythmias
University of Birmingham, UK | 03 – 04 September 2025

SA02

Cardiomyocyte microdomains: how local control of submembrane complexes drives cellular communication

Jose L. Sanchez-Alonso[1]

[1]Imperial College London, United Kingdom

Cell-to-cell communication in cardiomyocytes is mediated by specific signalosomes, protein complexes that play essential roles in regulating cellular responses. Cardiomyocytes are highly structured cells, and one key example of microdomain organization is the formation of a functional complex between β2-adrenergic receptors (β2ARs) and L-type Ca^{2+} channels (LTCCs) on the plasma membrane. However, the functional consequences of this microdomain localization remain incompletely understood. We found that LTCC activity is regulated by proximity coupling mechanisms exclusively via β2ARs—not β1ARs—highlighting a specific role for β2ARs in modulating LTCC response to adrenergic stimulation under healthy conditions. This coupling is lost in heart failure, both in rodent models and in humans, and is dependent on caveolin-3.

Cardiomyocytes also release nerve growth factor (NGF), which guides sympathetic neurons (SN) to form specialized contact sites with cardiomyocytes, termed neuro-cardiac junctions (NCJs). The formation of these NCJ microdomains induces significant physiological changes in cardiac cells. Using a co-culture model of human pluripotent stem cell-derived cardiomyocytes (hPSC-CMs) and SN, we demonstrated that SNs promote functional maturation of hPSC-CMs in vitro. Co-culture resulted in increased structural elongation, enhanced sarcomere organization, and improved force-frequency relationships—key features of mature cardiomyocyte function. Nicotine stimulation elicited a norepinephrine-dependent βAR response from SNs, leading to elevated cAMP production and enhanced contraction and Ca^{2+} transient amplitudes at baseline. Notably, this functional maturation did not extend to metabolic pathways.

Furthermore, SN co-culture increased action potential amplitude and depolarization velocity in hPSC-CMs, supporting a role for SNs in promoting electrophysiological maturation. Our findings suggest that neurons may influence cardiomyocyte expression of channels and receptors, including βARs, LTCCs, and Na^{+} channels (NaCh). We developed a novel patch-clamp technique that enables recording of voltage-gated channels in the cell-attached configuration on specific membrane regions, including the NCJ. Our data show that NCJs are enriched in NaCh-ankyrin G complexes, likely serving as anchoring structures between neurons and cardiomyocytes. The presence of NCJs also increased the number of LTCC/caveolin-3 complexes, suggesting that innervation actively reshapes the functional and electrophysiological landscape of cardiomyocytes.

In conclusion, our work underscores the critical role of submembrane protein complexes in both healthy and pathological cardiac states and highlights how NCJ formation drives functional changes mediated by these complexes.

Cross-Talk of Cells in the Heart 2025: Novel Mechanisms of Disease and Arrhythmias
University of Birmingham, UK | 03 – 04 September 2025

SA03

Regional specific changes in cardiac resident macrophages and fibroblasts modulate long-term atrial fibrillation maintenance

Ana Simon Chica[1], Jorge G. Quintanilla[1], Carlos Torroja[1], Peter Lee[2], Alberto Benguria[1], Concepción Revilla[3], Andres Redondo-Rodríguez[1], Estefanía Núñez[1], Javier Domínguez[4], Jesúz Vázquez[1], Manuel Carnero-Alcázar[5], David Filgueiras-Rama[1]

[1]Spanish National Center for Cardiovascular Research (CNIC), España, [2]Essel Research and Development Inc, Canada, [3]Departamento de Biotecnología, Centro Nacional Instituto de Investigación y Tecnología Agraria y Alimentaria, Spain, [4]Departamento de Biotecnología, Centro Nacional Instituto de Investigación y Tecnología Agraria y Alimentaria, España, [5]Cardiac Surgery Department, Hospital Clínico San Carlos, España

Most of the mechanistic insights into atrial fibrillation (AF) pathophysiology have been reported on cardiomyocytes, and it is commonly assumed that apply in the same manner to the atria as a whole. This study shows that atrial remodeling during persistent AF (PsAF) underlies differential adaptative changes in non-myocyte populations, which depend on the functional relevance of individual-specific atrial regions that sustain the overall arrhythmia (i.e., driver regions). Radiofrequency ablation at driver regions can terminate PsAF in pig models and achieve long-term AF-free survival in patients. Importantly, driver regions show overt compositional shifts in fibroblasts and myeloid populations that are highly consistent across pig models and patients. More specifically, driver regions are characterized by a phenotypic shift towards cardiac resident macrophages with an associated transcriptomic and proteomic profile favoring cardiomyocyte homeostasis and cell survival within a substrate prone to reentry. In fibroblasts, PTX3 represents a transcriptional hallmark exclusively present in driver regions, which supports their role on modulating regional specific changes during PsAF.

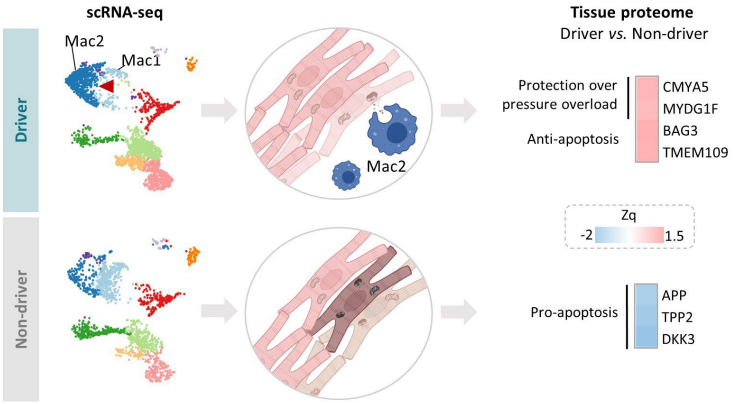

Cross-Talk of Cells in the Heart 2025: Novel Mechanisms of Disease and Arrhythmias
University of Birmingham, UK | 03 – 04 September 2025

SA04

Redefining catecholaminergic polymorphic ventricular tachycardia (CPVT) as a neurocardiac condition

Molly O'Reilly[1], Arie Verkerk[1], Carol Ann Remme[1]

[1]Amsterdam UMC - Academic Medical Centre, Netherlands

Background:

Catecholaminergic polymorphic ventricular tachycardia (CPVT) is an inherited arrhythmia syndrome caused by mutations in RYR2 (encoding ryanodine receptor 2, RyR2). Investigation into the pro-arrhythmic effects of these mutations have focused exclusively on cardiomyocytes. However, RyR2 is also present in neuronal tissue. Moreover, patients often present with clinical signs of autonomic nervous system (ANS) dysfunction, and treatment strategies frequently target the ANS.

Objective:

To assess whether RyR2 mutations affect the neurons that modulate cardiac function and/or impact on cardiac innervation, using an established CPVT mouse model (RyR2-R2474S).

Methods:

RNA sequencing, immunocytochemistry, live-cell fluorescence imaging, immunohistochemistry and liquid chromatography–mass spectrometry.

Results:

Analysis of published RNA sequencing datasets revealed that RyR2 is abundantly expressed in mouse stellate ganglia (SG; crucial autonomic modulators of cardiac function). Using immunocytochemistry, we confirm the presence of RyR2 protein in these peripheral, cardiac-modulating neurons. Functional investigation revealed a reduction of caffeine-induced calcium release in isolated CPVT SG neurons (Fura Red AM F/F0 CPVT 0.53±0.01 vs wild type (WT) 0.45±0.01; $p<0.01$), indicating the occurrence of intracellular calcium leakage. Moreover, cultured CPVT SG neurons showed increased neurite outgrowth (βIII tubulin/DAPI-positive area CPVT 6.9±0.6 vs WT 4.1±0.6 μm^2; $p<0.01$). Immunohistochemical staining of mouse heart cryosections with tyrosine hydroxylase (TH) demonstrated a significant increase in the density of sympathetic neuron innervation in ventricular tissue of CPVT mice (TH-positive area CPVT 3.8±0.5 vs WT 1.8±0.4 μm^2; $p<0.01$), and increased innervation heterogeneity (CPVT 5.4±1.3 vs WT 2.3±0.5 Δ μm^2; $p<0.05$). Neurotransmitter quantification in ventricular tissue revealed reduced levels of epinephrine in CPVT hearts (CPVT 0.023±0.002 vs WT 0.041±0.005 nmol/g; $p<0.01$), elevated levels of the norepinephrine (NE) metabolite normetanephrine (NMN), and a consequent increase in the NMN/NE ratio, which is an index of NE turnover (CPVT 0.26±0.02 vs WT 0.16±0.01 nmol/g; $p<0.05$). Quantification of blood plasma neurotransmitter metabolites revealed an increase in the dopamine metabolite 3-MT (CPVT 2.4±0.3 vs WT 1.3±0.2 nmol/g; $p<0.05$).

Conclusion:

The neurons that modulate cardiac function abundantly express RyR2. The RyR2-R2474S mutation leads to significant alterations of stellate ganglia neuron calcium homeostasis, increased neurite outgrowth, sympathetic hyperinnervation and increased innervation heterogeneity of ventricular myocardium, and

alterations of cardiac neurotransmitters and their metabolites. These functional and structural alterations of the ANS would have important consequences for cardiac function and arrhythmogenesis and may provide a novel blood biomarker for improved risk stratification and treatment design.

Cross-Talk of Cells in the Heart 2025: Novel Mechanisms of Disease and Arrhythmias
University of Birmingham, UK | 03 – 04 September 2025

SA05

Neurocardiac interactions in the human heart: defining heart highways

Cristina E. Molina[1]

[1]University Medical Center Hamburg –Eppendorf & University of Oxford, Germany/UK

Over the past decades significant progress has been made in understanding heart function, particularly in the context of excitation-contraction coupling and cardiac electrophysiology. These insights have provided a clear picture of the major pathophysiological mechanisms underlying cardiac diseases, including neurohormonal regulation of heart function. Nevertheless, understanding neurogenic mechanisms and the influence of neuronal remodelling on cardiac diseases onset and progression has been representing a challenging experimental problem. It is clear that cardiac autonomic alterations are extremely important in the pathogenesis of many cardiovascular diseases. This highlight the relevance of single-cell and cell-cell interaction studies to comprehensively delineate both individual cardiomyocyte and cardiac neuron function, as the crosstalk between the two of them. However, there is a profound gap of knowledge regarding the characterization of the neurons in the heart, in our understanding of this crosstalk and in how or whether cardiovascular targeted therapies impact on the activity of the neurons. We explore neurocardiac interactions using for the first time human cardiac myocytes and neurons.

Cross-Talk of Cells in the Heart 2025: Novel Mechanisms of Disease and Arrhythmias
University of Birmingham, UK | 03 – 04 September 2025

SA06

Disease-in-a-dish models to understand the mechanisms of atrial fibrillation in cardiomyopathies

Katja Gehmlich[1], Max Cumberland[2], Ashwin Roy[2], Andrew Holmes[3], Davor Pavlovic[2], Chris O'Shea[4], Richard Steeds[2]

[1] Cardiovascular Sciences, School of Medical Sciences, College of Medicine and Health, University of Birmingham and Division of Cardiovascular Medicine, Radcliffe Department of Medicine, University of Oxford, United Kingdom, [2]Cardiovascular Sciences, School of Medical Sciences, College of Medicine and Health, University of Birmingham, United Kingdom, [3]Department of Biomedical Sciences, School of Infection, Inflammation and Immunology, College of Medicine and Health, University of Birmingham, United Kingdom, [4]Cardiovascular Sciences, School of Medical Sciences, College of Medicine and Health, University of Birmingham and Heart Rhythm Research Group, Division of Biomedical Sciences, Warwick Medical School, Clinical Sciences Research Laboratory, United Kingdom

Atrial fibrillation is a common phenomenon in patients affected by inherited cardiac diseases, called cardiomyopathies. The traditional view is that structural remodelling, i.e. atrial enlargement and fibrosis, are responsible for this, however, novel observations suggest that atrial fibrillation may precede overt structural remodelling.

To get detailed insights into drivers of pro-arrhythmic changes, we have developed 'disease-in-a-dish' models for cardiomyopathies, making use of human induced pluripotent stem cell derived atrial cells. Our electrophysiological characterisation, using patch clamp and optical mapping approaches, has identified intrinsic changes in the electrical properties of atrial cardiomyocytes carrying key cardiomyopathy-associated mutations. Moreover, using 3D co-culture systems of atrial cardiomyocytes and cardiac fibroblasts, we can demonstrate that cross-talk between atrial cardiomyocytes and fibroblasts leads to fibroblast activation, a key event in fibrosis.

In conclusion, our models systems confirm the pro-arrhythmic characteristics of atrial cardiomyocytes and further provide an understanding of their mechanisms.

Cross-Talk of Cells in the Heart 2025: Novel Mechanisms of Disease and Arrhythmias
University of Birmingham, UK | 03 – 04 September 2025

C01

Validation of a mouse model of early chronic kidney disease-associated cardiomyopathy

Abbie Hayes [1], Katie Bruce[1], Michael Sagmeister[2], Jonathan Townend[1], Charles Ferro[1], Katja Gehmlich[1], Sophie Broadway-Stringer[1], Andre Ng[3], Rina Sha[1], Olivia Baines[1], Katie Tompkins[1], Rowan Hardy [2], Christopher O'Shea[1], Davor Pavlovic[1]

[1]Institute of Cardiovascular Sciences, University of Birmingham, United Kingdom, [2]Institute of Metabolism and Systems Research, Institute of Biological Research, University of Birmingham, United Kingdom, [3]Department of Cardiovascular Sciences, University of Leicester, United Kingdom

Introduction

Chronic kidney disease (CKD) affects 10–15% of the population globally [1]. Reduced kidney function can lead to CKD-associated cardiomyopathy, characterized by increased left ventricular mass, diastolic and systolic dysfunction, arrhythmias, and cardiac fibrosis. Our research shows that even individuals with moderate renal impairment exhibit cardiac structural changes [2] and are at risk of arrhythmias. Despite its high morbidity and mortality, CKD-associated cardiomyopathy remains poorly understood. This study explores the early mechanistic drivers of CKD-associated cardiomyopathy using a murine model induced by an adenine-rich diet.

Methods

8–12-week-old C57BL/6 mice were fed normal chow (male n=9, female n=9) or a 0.15% adenine diet (male n=16, female n=9) for up to 7 weeks. Blood plasma creatinine and urea were measured at sacrifice to assess kidney dysfunction. Kidney and cardiac tissue weights were recorded, and fibrosis was evaluated using histology and collagen 1 western blots. An O-link Target 48 proteomic cytokine panel assessed changes in serum levels of 45 cytokines.

Results

Adenine diet at 7 weeks significantly increased urea ($p < 0.0001$) in both males (adenine 27.91±5.385 mmol/L vs. control 8.84±0.786 mmol/L) and females (adenine 25.80±2.480 mmol/L vs. control 8.39±0.318 mmol/L). Creatinine also saw a significant increase ($p < 0.0001$) in both adenine males (adenine 48.89±3.434 umol/L vs. control 10.43±2.159 umol/L) and females (adenine 53.00±5.279 umol/L vs. control 14.86±1.184 umol/L). Kidney weight significantly decreased ($p<0.001$) in adenine-fed males (104.2 ± 4.600 mg) and females (190.2 ± 11.20 mg) compared to controls (155.8 ± 6.565 mg and 260.9 ± 8.957 mg, respectively). No significant changes in heart-to-body weight ratio were observed in adenine-fed mice (5.489 ± 0.3302 mg/g) compared to controls (5.307 ± 0.1096 mg/g). Histological evidence of fibrosis was observed in the right atrium (4.869 ± 0.5893% vs. 2.158 ± 0.3725%, $p < 0.0001$), left ventricle (2.866 ± 0.8118% vs. 0.8257 ± 0.1084%, $p < 0.01$), and left atrium (2.038 ± 0.2326% vs. 1.258 ± 0.1475%, $p < 0.05$) compared to controls. Western blots also detected an increased collagen 1 protein expression ($p<0.05$) in adenine fed mice. 39 of 45 proinflammatory cytokines were elevated in adenine fed mice, including biomarkers associated with cardiomyopathy, such as Ccl5, Ccl11, and Ffgf21.

Conclusion

The adenine diet induced early CKD-associated cardiomyopathy, characterized by cardiac fibrosis and systemic inflammation, without significant changes in heart weight [3]. Our ongoing work is examining the haemodynamic changes, in vivo ECG and electrical changes in the heart.

Cross-Talk of Cells in the Heart 2025: Novel Mechanisms of Disease and Arrhythmias
University of Birmingham, UK | 03 – 04 September 2025

C02

Development and characterisation of a 3D epicardial cardiac model

Kenza Sackho[1], Justin Duruanyanwu[1], Rahme Safakli[1], Ioannis Smyrnias[2], Akram Jawad[3], Youngchan Kim[3], Paola Campagnolo[2]

[1]School of Biosciences, Faculty of Health & Medical Sciences, University of Surrey, Guildford GU2 7XH, UK, United Kingdom, [2]School of Veterinary Medicine, Faculty of Health and Medical Sciences, University of Surrey, Guildford GU2 7XH, UK, United Kingdom, [3]Advanced Technology Institute, University of Surrey, Guildford GU2 7XH, UK, United Kingdom

INTRODUCTION: The epicardium provides progenitor cells and paracrine signals crucial for cardiac development and repair (1) . Despite its reported dormant status in adulthood, the adult epicardium reactivates in response to cardiac damage to provide pro-reparatory signals, influencing both cardiomyocytes and endothelial cells (1) . Enhancing the reparative potential of the epicardium represents an interesting novel route of intervention, but the paucity of adult in vitro epicardial models hampers progress (2). Advancing models that integrate epicardial cells with other cardiac cell types will be critical for dissecting cell-cell crosstalk in adults in both homeostasis and disease.

AIMS: Develop a 3D epicardial model, characterise this model using a variety of imaging techniques.

METHODS: This project engineered a multicellular heart spheroid model inclusive of the epicardial layer. Cardioids were formed with cardiomyocytes (rat neonatal or H9C2), fibroblasts (rat neonatal or human), and human endothelial cells in a 12,000:12,000:12,000 ratio. Two epicardioids models were developed that consisted of either 1,000 adult pig epicardial cells (EPDCs) or mouse embryonic epicardial cells (MECs). These ratios were chosen to mimic the in vivo composition. Spheroids were optimized for cell ratio and culture conditions and subsequently characterized via bright field and confocal microscopy. Structural organisation of cell types was determined using immunostaining (CD31,MSLN and connexin-43) and viability was assessed with both live dead staining and metabolic activity assays. To determine activity of cells within the spheroids they were challenged with pro-fibrotic TGF-β1 and hypertrophy stimuli such as phenylephrine (PH) and outcomes were assessed via immunostaining and qPCR.

RESULTS: Spheroids formed most robustly at 1:1:1 ratio of rat fibroblasts and cardiomyocytes, and human endothelial cells in cardiomyocyte media yielded spheroids with no central translucency following 3 days of culture. Addition of 1,000 epicardial cells at time 0 resulted in the most intact epicardial layer, showcased by fluorescence imaging. EPDCs epicardioids were smaller than cardioids ($P \leq 0.05$), indicating that epicardial cells confers compactness. CD31 and MSLN staining showcased organized endothelial layering suggestive of coronary-like structures. H9C2 myoblasts viability was preserved in EPDC epicardioids as compared to MEC epicardioids ($P \leq 0.01$). MEC epicardioids displayed 59% more endothelial cells compared to cardioids ($P \leq 0.001$) and 49% more than EPDC epicardioids ($P \leq 0.01$), suggesting a pro-angiogenic role of embryonic epicardial cells. Additionally, adult epicardial cells promoted healthy H9C2 morphology compared to Cardioids. Challenge with TGF-β1 resulted in increased collagen expression, a marker of fibroblast activation and enhanced cellular release, as confirmed by immunostaining and qPCR analysis. PH treatment determined a marked trend of increased nuclear area, indicative of hypertrophy.

DISCUSSION & CONCLUSIONS:

Epicardioids offer a novel platform to study adult epicardial communication with the main cell types of the heart. Recapitulating key aspects of epicardial interaction with myocardial and endothelial populations showcased by the structural organisation of endothelial structures and distinct morphological changes in H9C2 cells the presence of adult epicardial cells. This model enables functional assessment of epicardial influence on cardiac remodelling and may accelerate discovery in cardiac regeneration, drug screening, and disease modelling.

C03

Multicellular Modelling of Tumour Necrosis Factor-α Driven Cardiac Dysfunction in Human Engineered Heart Tissues and Myocardial Slices

Fatemeh Kermani[1], Anna Son[1], Mary Ball[1], Lynn Li[1], Cesare Terracciano[1]

[1]Imperial College London, United Kingdom

Heart failure (HF) represents the end-stage phenotype of various cardiac pathologies, including hypertension, ischemic heart disease, diabetes, and cardiomyopathies. In response to cardiac stress, activation of the innate immune system triggers the secretion of pro-inflammatory cytokines, including tumor necrosis factor-alpha (TNF-α). Chronic inflammation contributes to adverse cardiac remodeling and progressive ventricular dysfunction. Animal studies have reported that elevated TNF-α levels are associated with cardiac dilation, fibrosis, and contractile dysfunction (1,2). However, due to species differences, findings from animal models may not always translate directly to humans.

In vitro studies indicate that TNF-α overexpression in human induced pluripotent stem cell–derived cardiomyocytes (hiPSC-CMs) induce apoptosis and impair Ca^{2+} cycling. This oxidative stress–driven dysfunction ultimately leads to reduced contractile amplitude (3,4). While such studies provide valuable insight into the effect of TNF-α on CMs, these models lack physiological relevance. hiPSC-CMs exhibit a neonatal-like phenotype, which may respond differently to TNF-α compared to adult CMs. Moreover, in the human heart, CMs are in interaction with non-cardiomyocytes, including fibroblasts (FBs) and endothelial cells (ECs). These cell–cell interactions likely influence CM responses to TNF-α, yet they are often not considered in traditional in vitro models.

This study aims to address that gap by investigating the effect of TNF-α in tri-culture engineered heart tissues (EHTs) and human living myocardial slices (LMS). Briefly, hiPSC-CMs, cardiac FBs, and human cardiac microvascular endothelial cells (hCMVECs) were used to generate EHTs. These were treated with 100 ng/mL TNF-α for one week. EHTs were electrically paced at 1 Hz, Ca^{2+} kinetics were measured using live Ca^{2+} imaging, and contractility was assessed via video-based motion analysis. For statistical analysis, data were tested for normality, and an unpaired t-test was applied.

Human donor hearts were provided by the NHS Blood and Transplant INOAR program (IRAS project ID: 189069), with approval from the NHS Health Research Authority and in compliance with the Governance Arrangements for Research Ethics Committees. LMS were generated from the left ventricle of donor human hearts (dimensions: 8 mm × 8 mm × 0.3 mm). Slices were cultured in chambers—one as a control, and the other treated with TNF-α and electrically stimulated during culture (1 Hz, 10 V, 10 ms pulse duration). After two days, contractile function was assessed. To determine whether TNF-α induces arrhythmogenic activity, LMS were paced at 2 Hz for 30 seconds, followed by a 2-minute pause to monitor for spontaneous contractions.

Our data show that TNF-α–treated EHTs exhibited a significantly higher spontaneous beating rate and reduced contraction amplitude ($n=8\text{-}10/ p<0.05$), although no changes in Ca^{2+} handling were observed. Additional replicates are required to confirm these findings. Consistently, TNF-α–treated LMS showed a significant reduction in active force, increase in passive force and slices developed arrhythmic events ($n= 10\text{-}12/ p<0.001$).

In summary, TNF-α impairs contractile function and induces arrhythmias in both EHT and LMS. These findings underscore the pathological role of TNF-α in human cardiac tissue and emphasize the importance of physiologically relevant platforms to study inflammation-driven heart failure. Further

investigation is needed to elucidate the underlying signaling mechanisms and explore potential receptor-specific therapeutic strategies.

C04

Age-Associated Loss of Lymphatic Vessels Promotes Cardiac Inflammation

Julian Wagner[1], Hamza Gulshan[1], Ibrahim Sultan[2], Salli Antila[2], Laia-Canes Esteve[3], David Rodrigues Morales[1], Emmanouil Solomonidis[1], Simone-Franziska Glaser[1], Wesley Abplanalp[1], Tara Procida-Kowalski[4], Marek Bartkuhn[4], Evelyn Ulrich[5], Sarmad Ahmad Khan[5], Jochen Pölling[3], Thomas Braun[3], Kari Alitalo[2], Stefanie Dimmeler[5]

[1]Goethe-University Frankfut, Germany, [2]University of Helsinki, Finland, [3]Max-Planck-Institute for Heart and Lung Research, Bad Nauheim, Germany, [4]Justus-Liebig-University Giessen, Germany, [5]Goethe-University Frankfurt, Germany

Introduction: Aging is a major risk factor for cardiovascular diseases. One prominent hallmark of cardiac aging is inflammation. The microcirculatory system and age-related immune cell infiltration has been extensively studied in this context, however, the contribution of the lymphatic vasculature to age-related pathologies remains elusive.

Methods: To assess the cardiac lymphatic system, whole mount light sheet microscopy and confocal imaging was used. Functional alterations were investigated using AAV9 coding for Vegfc or soluble Ft4 were injected into 18-month-old and 3-month-old mice, respectively. Flt4;prox1-CreERT2 mice were used as additional model. Finally, molecular mechanisms were characterized using snRNA-seq on aged AAV9-Vegfc treated mcie.

Results: We examined lymphatic capillary density in old (>20 months) and young (3 months) mouse hearts using LYVE1 and PDPN staining. Aging induced a significant decline in lymphatic vessel density in the sub-endocardial and -epicardial area of aged left ventricles in both genders (0.28±0.08 fold and 0.68±0.03 fold; $p<0.05$), while the right ventricle showed no change. Dilation of peri-arterial lymphatics was observed in old hearts, indicating lymphatic drainage dysfunction. Cardiac aging was accompanied by increased numbers of CD68+ macrophages, accumulation of fibrinogen and amyloid in the interstitial space, and significant tissue edema ($p<0.05$). The decline in lymphatic vessels was associated with reduced Vegfc expression (0.72±0.04 fold; $p<0.005$) in aged hearts.

To establish a causal link, we examined hearts from 3-month-old Flt4;Prox1-CreERT2 mice with defective lymphatic vessels. These mice displayed fibrinogen (1.32±0.08 fold; $p<0.05$) and CD68+ macrophage (1.58±0.08 fold; $p<0.05$) accumulation compared to wildtype littermates. Blocking VEGFC signaling in young mice by overexpressing soluble Flt4 impaired cardiac lymphatic capillary density (0.62±0.06 fold; $p<0.01$), leading to increased macrophage and fibrinogen accumulation (1.69±0.09 fold, 4.60±0.30 fold; $p<0.001$) and diastolic dysfunction.

We then addressed whether restoring Vegfc expression in old mice rescues age-related cardiac impairment. Inducing Vegfc via AAV9 in aged mice restored cardiac lymphatic density by 3-fold and reduced CD68+ macrophage density by 1.6-fold, without affecting fibrinogen accumulation. However, overexpression of Vegfc lead to cardiac fibrosis and transiently impaired diastolic function.

Conclusion: Our study demonstrates an age-related reduction in left ventricular lymphatic density, cardiac edema, and inflammation. Vegfc overexpression prevented age-dependent decline of lymphatic vasculature and reduced cardiac inflammation.

Cross-Talk of Cells in the Heart 2025: Novel Mechanisms of Disease and Arrhythmias
University of Birmingham, UK | 03 – 04 September 2025

C05

The role of small extracellular vesices in myocardial hypoxia-reoxygenation injury studied with living myocardial slices

Fani Koutentaki[1], Linjie Zheng[1], Richard Kelwick[1], Paul Freemont[1], Cesare Terracciano[1]

[1]Imperial College London, United Kingdom

Extracellular vesicles (EVs) play a regulatory role in the progression of cardiovascular disease. Myocardial ischaemia-reperfusion injury (IRI) induces an increase in the secretion of small extracellular vesicles (sEVs) in the cardiac microenvironment and peripheral circulation(1). sEVs are lipid bilayer particles within the size range of 35-200nm and secreted by all cell types. Their high content of bioactive molecules – primarily microRNA – is altered in response to external stimuli, leading to behavioral changes of the recipient cells. Studies have shown that cultured cardiomyocytes (CMs) produce exosomes that monitor cardiovascular events in response to IRI in a murine model(2). sEVs produced by stem cell-derived endothelial cells subjected to hypoxia carried a miR that inhibited apoptosis and stimulated angiogenesis, increasing CM survival and contractility in a human IRI heart-on-a-chip model(3).

The mechanism behind altered sEV secretion and their changes in content in cardiovascular disease had not been determined due to lack of models. The human living myocardial slice (LMS) in vitro model maintains the cellular complexity of the myocardium, providing a platform for the isolation of sEVs and allowing the investigation of the changes in sEV concentration and content(4).

The present work aims to employ a new LMS model of IRI to characterize the process of sEV secretion and uptake, and the consequences on the functional, structural and biochemical properties of the myocardium. Human donor hearts are provided by the NHS Blood and Transplant INOAR program with approval from the NHS Health Research Authority (IRAS project ID: 189069), and in compliance with the Governance Arrangements for Research Ethics Committees. The LMSs are subjected to continuous electrical stimulation (1 Hz) and mechanical load (preload 22% stretch); they are exposed to hypoxia-reoxygenation injury (HRI) by being placed in a hypoxic chamber set at 1% O2 concentration for 2 hours, followed by 24 hours of reoxygenation. After culture, a force transducer is used to measure contraction kinetics at different stretches of the LMS. sEVs are isolated by size exclusion chromatography and their concentration is determined by Nanoparticle Tracking Analysis. Statistical analysis is performed with a 2-way ANOVA with Tukey's multiple comparisons test.

LMSs subjected to HRI at 1% O2 for 2 hours show a significant reduction in force transient amplitude at 20%, 22%, 25%, and 30% sarcomere length ($p=0.0109$, $p=0.0039$, $p=0.003$, $p=0.002$ respectively, $N=4$) compared to healthy LMSs. In fact, the force transient amplitude of the HRI LMSs decreases by 47% ($p<0.0001$). Additionally, the quantification of sEVs shows a significant increase in sEV concentration following HRI ($p=0.0454$, $N=4$). Future plans include the immunohistochemistry staining of the LMS HRI and sEVs, and the molecular analysis of the microRNA content of sEVs. In summary, the exposure of human LMSs to 1% hypoxia for 2 hours followed by 24 hours reoxygenation affects their function and induces the increased secretion of sEVs.

In conclusion, we have established a reliable human LMS model to investigate the role of sEVs in response to HRI. The molecular analysis of sEV content will allow identification of novel biomarkers and potential therapeutic targets of cardiovascular disease.

Cross-Talk of Cells in the Heart 2025: Novel Mechanisms of Disease and Arrhythmias
University of Birmingham, UK | 03 – 04 September 2025

C06

Neurocardiac interactions using hiPSC derived cardiomyocytes and sympathetic neurones from CPVT patients

Yoon Young Choi[1], Ni Li[1], Dan Li [1], David J. Paterson[1]

[1]Department of Physiology, Anatomy and Genetics, University of Oxford, United Kingdom

Background: Catecholaminergic Polymorphic Ventricular Tachycardia (CPVT) is a rare but life-threatening inherited arrhythmic disorder, typically triggered by exercise or emotional stress, and a leading cause of sudden cardiac death in the young. CPVT is commonly caused by mutations in calcium-handling components of sarcoplasmic reticulum (SR), which promote diastolic calcium leakage and increase arrhythmogenic risk under adrenergic stress. Current therapies such as β-blockers and, in more severe cases, cardiac sympathetic denervation, remain insufficient in a significant subset of patients – suggesting a more complex pathophysiological mechanism. Although previous studies have characterised CPVT phenotypes in human induced pluripotent stem cell-derived cardiomyocytes (hiPSC-CMs), the contribution of diseased sympathetic neurones (SNs) to the CPVT phenotype remains poorly understood.

Method: hiPSCs derived from both a CPVT patient and a healthy control were differentiated into cardiomyocytes (hiPSC-CMs) and sympathetic neurones (hiPSC-SNs). Electrophysiological activity was assessed using multi-electrode array (MEA) recordings. Calcium transients were measured using Fura-2AM indicator. Real time cAMP dynamics were monitored using a fluorescence resonance energy transfer (FRET) based biosensor (Epac-S^{H187}). All hiPSC lines used in this study were ethically approved and obtained from established sources with appropriate donor consent.

Results: To characterise features of baseline cardiac action potential, MEA measurements were conducted. At baseline, 47% (8 out of 17) of CPVT hiPSC-CMs exhibited spontaneous arrhythmic activity, including tachycardia and re-entry phenomena, compared to none in controls (n=8). Among regularly beating cells, CPVT hiPSC-CMs showed significantly shorter RR intervals (control: 0.5638±0.049s, n=8; vs CPVT: 0.4412±0.025s, n=8; unpaired t-test; $p<0.05$) and field potential durations (control: 0.3406±0.041s, n=8; vs CPVT: 0.1844±0.015s, n=8; unpaired t-test; $p<0.01$). Application of isoprenaline (β-adrenergic stimulation) shortened RR interval in both groups. Arrhythmias were triggered in some CPVT cardiomyocytes (regular at baseline), but not in controls. Calcium imaging revealed greater isoprenaline-induced calcium transients in CPVT hiPSC-CM (Control: 0.05±0.01, n=11; vs CPVT: 0.99±0.13, n=14; unpaired t-test, $p<0.05$). Spontaneous calcium discharges were detected in 77.4% (24 out of 31) of CPVT compared to 10% (1 out of 10) of controls. FRET analysis showed significantly elevated cAMP responses in CPVT hiPSC-CM following isoprenaline stimulation (control: 48.63±1.625%, n=98; vs CPVT: 64.25±1.990%, n=70; Mann-Whitney test; $p<0.0001$). For hiPSC-SN, CPVT displayed enhanced calcium transients and elevated cAMP elevation following nicotine stimulation, compared to isogenic controls. In hiPSC neurocardiac co-culture, nicotine stimulation increased the beating rate of cardiomyocytes, confirming functional connectivity. The reduction in RR interval was significantly greater in control cardiomyocytes co-cultured with CPVT neurones (n=5) than with control neurones (n=4, Mann-Whitney test; $p<0.05$). Calcium imaging showed that CPVT hiPSC-SN consistently exhibited elevated calcium transients, regardless of cardiomyocyte genotype they were paired with. This indicates that hyperactivity of neurones is intrinsic and not modulated by co-cultured cardiomyocytes.

Conclusion: Our investigation confirms hallmark CPVT abnormalities in hiPSC-CMs, including arrhythmia, calcium dysregulation and altered β-adrenergic cAMP signalling. Additionally, our results suggest a novel pathogenic role for CPVT sympathetic neurones, whose intrinsic hyperactivity exacerbates the cardiomyocyte phenotype via neurocardiac cross-talk. These findings provide new insights into the pathophysiology of CPVT and highlight the potential of targeting sympathetic excitability as a therapeutic strategy for personalised treatments.

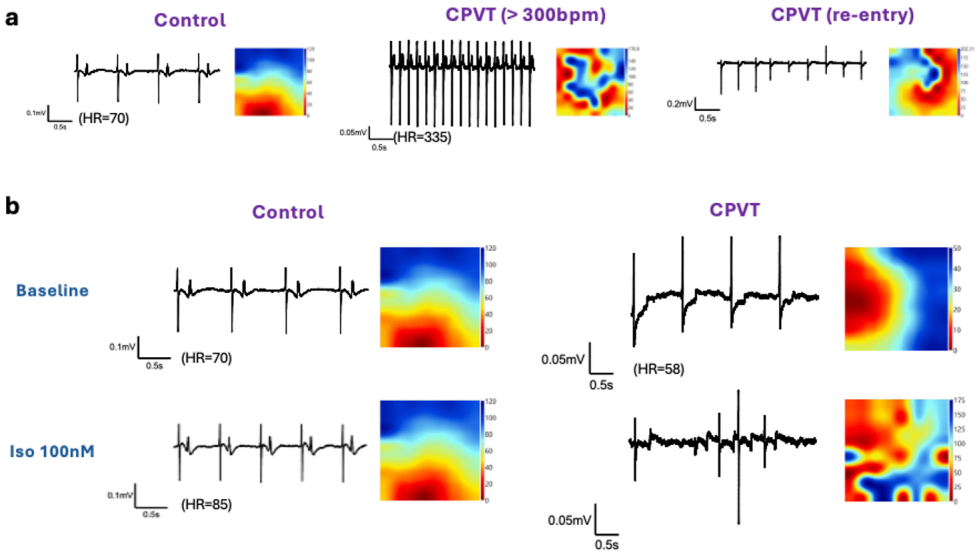

Figure 1. Field potential traces and activation maps of control and CPVT hiPSC-CMs using multi-electrode array (MEA) recordings. a: Baseline field potential traces of control and CPVT hiPSC-CMs. CPVT traces show examples of tachycardia (>300bpm) and re-entry phenomenon, while control trace exhibits regular rhythm. **b:** Representative traces following isoprenaline (Iso) stimulation. Arrhythmias were triggered in a subset of CPVT cardiomyocytes that were regularly beating at baseline, but not in controls.

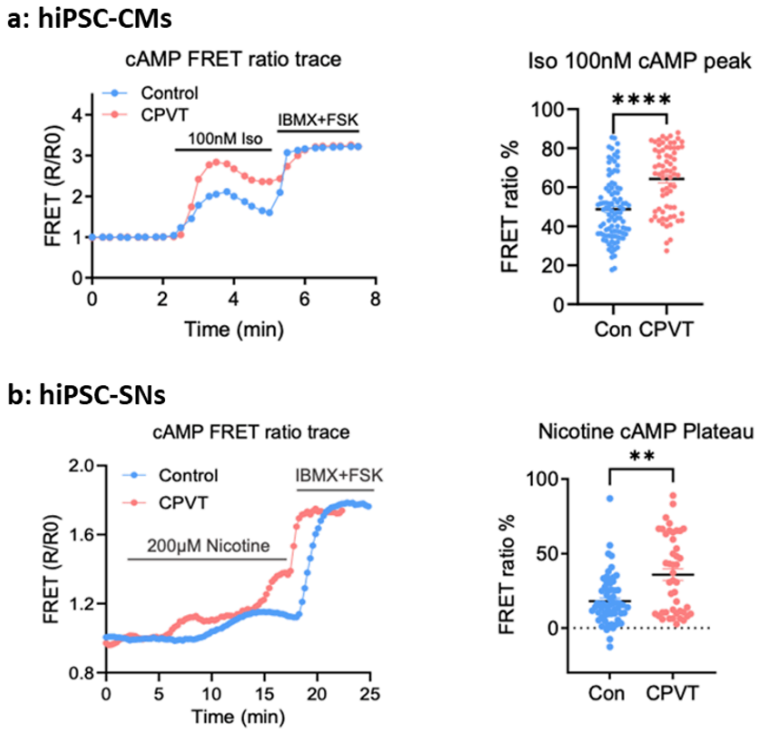

Figure 2. cAMP FRET measurements in control and CPVT hiPSC-CMs and hiPSC-SNs. **a:** Representative FRET traces in hiPSC-CMs showing responses to 100nM isoprenaline (Iso) added at 2-minute, and IBMX + forskolin (FSK) added at 5-minute to saturate the FRET sensor. FRET ratio % was calculated as the change in FRET signal (R/R_0) upon Iso stimulation, normalised to the maximal response induced by IBMX + FSK. CPVT hiPSC-CMs exhibited significantly elevated cAMP responses compared to controls (control: n=98 vs CPVT: n=70; Mann-Whitney test; $p<0.0001$). **b:** Equivalent FRET traces and quantification in hiPSC-derived sympathetic neurones (hiPSC-SNs) following 200 μM nicotine stimulation and subsequent IBMX + FSK addition. CPVT neurones demonstrated significantly greater cAMP responses than control neurones (control: n=63 vs CPVT: n=45; Mann-Whitney test; $p<0.01$).

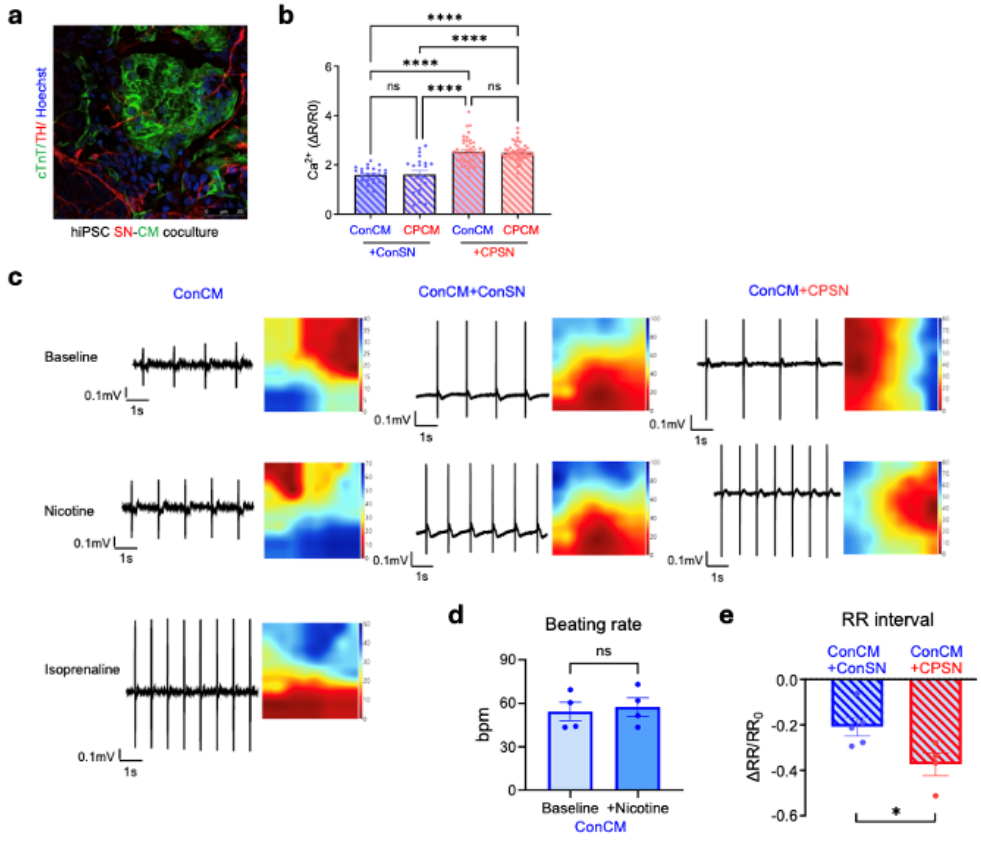

Figure 3. Calcium signalling and electrophysiological properties of hiPSC-derived neurocardiac co-cultures. a: Immunofluorescence showing co-localisation of cardiac (cTnT) and sympathetic neuronal (TH) markers in co-culture. The overlay highlights the interspersion of neuronal projections among cardiomyocytes. **b:** Calcium transient amplitudes ($\Delta R/R_0$) in sympathetic neurones (SNs) co-cultured with control (ConCM) or CPVT (CPCM) cardiomyocytes. Following stimulation with high-potassium (50mM), CPVT sympathetic neurones (CPSN) showed significantly higher calcium release than control neurones (ConSN), regardless of the cardiomyocyte genotype. **c:** Representative field potential traces and activation maps showing electrical activity in hiPSC-CMs in monoculture and co-culture with SNs. 100 μM nicotine had minimal effect on beating rate in monocultures but induced a marked increase in the beating rate in co-culture, confirming functional connectivity. Isoprenaline 1μM served as a positive control. **d:** Group data showing that 100 μM nicotine had no significant alteration in beating rate in control hiPSC-CM monocultures. **e:** Change in RR interval ($\Delta RR/RR_0$) in ConCM co-cultured with either control (ConSN) or CPVT sympathetic neurones (CPSN) in response to nicotine stimulation. Co-culture with CPSN (n=5) resulted in significantly greater RR interval shortening compared to ConSN (n=4, Mann-Whitney test, $p < 0.05$).

Cross-Talk of Cells in the Heart 2025: Novel Mechanisms of Disease and Arrhythmias
University of Birmingham, UK | 03 – 04 September 2025

C07

Aging-Induced Sympathetic Hyperinnervation is Specific to the Left Atrium

Annika Maria Theresa Braun[1], Sebastian Clauß[2], Shasha Zhu[2], Ruibing Xia[2], Veronica Larcher[1], Denada Arifaj[1], Katja Schmitz[1], Thomas Körtl[3], Samuel Tobias Sossalla[3], Stefanie Dimmeler[1], Julian Uwe Gabriel Wagner[1]

[1]Institute of Cardiovascular Regeneration, Goethe University Frankfurt, Germany, [2]Department of Medicine I, University Hospital Munich, Ludwig Maximilian University, Deutschland, [3]Department of Medicine I, University Hospital Gießen Marburg, Kerckhoff Campus, Bad Nauheim, Germany

Introduction: With increasing life expectancy, age-related diseases emerged as a leading cause of mortality. The aging myocardium is characterized by structural/functional alterations, which predispose the elderly to arrhythmias. The autonomic nervous system (ANS) and neurovascular interactions recently gained increasing attention, as previous findings demonstrate that endothelial senescence induced denervation of the left ventricle (LV) in aging. However, the effects of aging on atrial innervation and neurovascular cross-talks remains unexplored. Since alterations of the ANS increases the risk of atrial fibrillation (AFib), which is highly prevalent in the elderly, we explored the innervation and the neuro-vascular cross-talk in the aging atria.

Aims/Objectives: In this project we aim to study age-related changes in atrial innervation and possible impact on arrhythmias.

Methods: To characterize the ageing murine atria, we used immunofluorescence-based stainings and senolytic experiments. Further, we included single-nuclei RNA sequencing and in vivo electrical pacing experiments. Burst stimulation protocol for atria was used to provoke atrial arrhythmias.

Results: To investigate atrial innervation in aged hearts, we stained pan-neuronal marker beta-3-tubulin in LAs of 3-months-old and 22-months-old mice, observing a 1.6±0.1-fold increase (p=0.0141 (unpaired, parametric t-test), 3m n=8, 22m n=6)) in aged mice, while innervation decreased in the LV. This increase in LA innervation was primarily attributed to enhanced sympathetic innervation, with a 1.6±0.1-fold increase (p=0.0003 (unpaired, parametric t-test), 3m n=13, 22m n=8)) as determined by tyrosine-hydroxylase staining.

Since we previously found that vascular senescence controls denervation of the LV, we investigated cellular senescence patterns between the LV and the LA. Acid β-galactosidase staining showed a 3.4±0.1-fold increase (p=0.001 (unpaired, parametric t-test), 3m n=11, 22m n=8) in LA senescence with age. However, double staining with cell type specific markers revealed no increase in endothelial cell senescence but a tendency for increased senescence in CD45-positive immune cells (2.7±0.1-fold increase, p=0.0964 (unpaired, parametric t-test), n=8) and CD68-positive macrophages (2.9±0.1-fold increase, p=0.0585 (unpaired, parametric t-test), n=8).

Consistent with these findings, treating mice with the endothelial cell specific senolytic drug fisetin did not affect LA senescence or hyperinnervation in aged LAs after 2 months of treatment but reduced cellular senescence in the LV. These data indicate that LA hyperinnervation in aging is associated with immune cell but not endothelial cell senescence.

To investigate mechanisms underlying LA hyperinnervation, we performed single-nuclei RNA sequencing. First analyses demonstrate that macrophages show an increased neuroinflammation signature in aged

murine LAs. Cell types like endocardial endothelial cells on the other hand showed a more pro-axon guidance phenotype with declined axon-repelling factors such as SEMA3A, while protective factors such as VEGFB were increased.

Preliminary results of electrical pacing experiments in young and 16-months-old mice revealed that aged mice have a higher susceptibility for induced AFib compared to young counterparts. This suggests that LA hyperinnervation might be associated with AFib. Histological analysis of LA samples from human patients (n=3) confirmed high innervation levels in AFib.

Conclusions: In conclusion, we demonstrate hyperinnervation in aged LAs. Future research will focus on the relationship between AFib and LA hyperinnervation while unraveling the molecular mechanisms driving these age-related changes.

Cross-Talk of Cells in the Heart 2025: Novel Mechanisms of Disease and Arrhythmias
University of Birmingham, UK | 03 – 04 September 2025

C08

Investigating the role of IKs and IKr in the electrophysiological responses to sympathetic nerve stimulation in an innervated isolated rabbit heart model

Rachel Sutcliffe[1], Bethan Roper-Jones[1], Emily Allen[1], Reshma Chauhan[1], Andre Ng[2]

[1]University of Leicester, UK, [2]University of Leicester, Leicester British Heart Foundation Centre of Research Excellence, Leicester National Institute for Health and Care Research Biomedical Research Centre, UK

Introduction

Sympathetic nerve stimulation(SNS) shortens ventricular action potential duration(APD), ensuring diastolic filling despite increased heart rate(HR). This shortening has been reported to be driven by sympathetically sensitive IKs and IKr currents. SNS is known to increase the risk of sudden cardiac death through an increased incidence of ventricular fibrillation(VF) linked to the heterogenous effects of SNS on ventricular electrophysiology caused by regional differences in nerve and ion channel distribution. The effects of IKr and IKs blockade on this heterogeneity, and on the electrophysiological effects of SNS, have not been studied in detail in the rabbit ventricle.

Methods

An innervated isolated rabbit (NZW 3.38± 0.05kg, initial sedation (subcutaneous Sedator-0.2mg/kg, Ketavet-10mg/kg), followed by surgery under intravenous propofol before terminal anaesthesia (Dolethal – 160mg/kg)) was used to examine left ventricular (LV) APD responses to SNS during pacing. Protocols were run initially without drug, followed by pharmacological blockade of IKs (0.5μM HMR, n=6) or IKr(0.03μM E4031, n=7) and finally with blockade of both IKr and IKs combined(0.5μM HMR and 0.03μM E4031)

Results

Both LV apical and basal APDs were lengthened by E4031 (110±5ms to 133±5ms, $p<0.001$; 118±5ms to 146±10ms, $p<0.05$) and were modestly but not significantly lengthened with HMR (118±3ms to 127±5ms;119±7ms to 128±5ms). Similarly, both LV apical and basal APDs were lengthened significantly by the addition of E4031 to HMR (140±6ms, $p<0.01$; 163±8ms, $p<0.01$), and more modestly by the addition of HMR to E4031(150±11ms; 151±10ms). In all cases, SNS shortened both apical and basal APD, but the magnitude of this SNS-induced shortening was almost always greater in the base.

The effective refractory period (ERP) was also lengthening with HMR and to a greater extent with E4031(135±4ms to 146±4ms, $p<0.01$; 127±6 to 170±8ms, $p<0.01$). SNS significantly shortened ERP both in the absence and presence of HMR (120±4ms, $p<0.001$; 131±7ms, $p<0.01$) and E4031(116±3ms, $p<0.05$; 145±6ms, $p<0.01$). While the magnitude of this SNS-induced shortening was the same with or without HMR(-10.7% to -10.4%), it was significantly increased by E4031(-8.1% to -14.6%, $p<0.5$). ERP was not compared with both drugs combined, as the protocol often induced ventricular fibrillation(6/16 hearts).

Despite the high incidence of VF during ERP protocols with both drugs we saw no significant changes in VFT with HMR, E4031 or both drugs combined. In addition, the magnitude of the SNS-induced reduction in VFT was not significantly altered by these pharmacological blockades.

Conclusion

In this study, we observed greater APD and ERP lengthening with E4031 than with HMR and an increase in SNS-induced ERP shortening only with E4031. These results reflect the known variation in the roles of IKs and IKr in both the rabbit ventricle and in the sympathetic response. Despite a noticeable increase in the incidence of VF with both drugs combined during our ERP protocol, we didn't observe any significant changes in VFT in this study, perhaps a result of the protocol used. In addition, when both IKr and IKs were pharmacologically blocked, the SNS-induced APD shortening and VFT reduction were still present, suggesting that in these experiments, some repolarisation reserve remains.

Cross-Talk of Cells in the Heart 2025: Novel Mechanisms of Disease and Arrhythmias
University of Birmingham, UK | 03 – 04 September 2025

C09

Generation of an engineered heart tissue model of Hypertrophic Cardiomyopathy, caused by MYBPC3 R820W mutation

Mary Ball[1]

[1]Imperial College London, United Kingdom

Introduction: Hypertrophic cardiomyopathy (HCM) is a disease that affects 3 in 20 cats and 1 in 500 humans [1]. The MYBPC3 R820W mutation causes HCM in ragdoll cats and humans [2], and is characterised by cardiomyocyte (CM) remodelling, myofiber disarray, interstitial fibrosis, left ventricular hypertrophy and hypercontractility. Despite some breakthrough drugs such as Mavacamten, there are limited treatments available to reverse all aspects of HCM, such as interstitial fibrosis [3]. The exact pathological mechanisms leading to HCM caused by the MYBPC3 R820W mutation have not been studied in detail. However, they likely involve interactions between dysfunctional CMs and other cardiac cells, including cardiac fibroblasts (CFs) [4, 5]. Our lab has generated a novel induced pluripotent stem cell (iPSC) line homozygous mutant for the MYBPC3 R820W mutation (R820W+/+), and an isogenic control line.

Our overall aim for this project was to generate an engineered heart tissue (EHT) model of HCM and use it to understand the aberrant interactions between R820W+/+ iPSC-derived CMs (iPSC-CMs) and CFs. Our objectives were:

- To use a novel ImageJ and R script to measure differences in contractility parameters between EHT groups.
- To use immunohistochemistry to measure differences in iPSC-CM area (hypertrophy), iPSC-CM alignment and fibrosis.

Methods: We generated EHTs containing R820W+/+ or isogenic control iPSC-CMs, either alone or with CFs (n=5-10 per group). EHTs were cultured for 2 weeks, then electrically stimulated at 1Hz and 10 second videos were taken to measure contractility. Then EHTs were either fixed for staining or processed for RNA and protein extraction. Two-way ANOVA was used for all statistical analyses.

Results: EHTs with CFs showed a significantly shorter time to peak of contraction and contraction duration compared to EHTs with iPSC-CMs only, regardless of iPSC-CM mutation ($p<0.0001$ isogenic control, $p=0.0093$ R820W+/+). R820W+/+ EHTs with iPSC-CMs only had a significantly shorter time to peak of contraction compared to isogenic control EHTs with iPSC-CMs only ($p=0.0363$). Also, R820W+/+ EHTs with iPSC-CMs and CFs had a significantly shorter relaxation time, compared to the R820W+/+ EHTs with iPSC-CM only. For iPSC-CM area, results revealed a larger iPSC-CM area in R820W+/+ EHTs with CFs, compared to isogenic control EHTs with CFs. For iPSC-CM alignment, we found that adding CFs to isogenic control EHTs caused significantly more iPSC-CM alignment, compared to isogenic control EHTs with iPSC-CMs only ($p<0.0001$). Also, R820W+/+ EHTs with CFs showed significantly less iPSC-CM alignment, compared to the isogenic control EHTs with CFs ($P=0.0186$). Analysis of Masson's trichrome staining showed no significant difference in fibrosis between groups ($P>0.05$).

Conclusions: our model of HCM shows a mild hypercontractile phenotype, which is ameliorated by the addition of CFs. Our results also show the expected interactions between isogenic control iPSC-CMs and CFs, indicating that the model is working. We have revealed a possible interaction between R820W+/+ iPSC-CMs and CFs which leads to hypertrophy and myocardial disarray. Future work will focus on

investigating differences at the protein and gene level, and maturing the EHT model further with electrical stimulation in culture.

Cross-Talk of Cells in the Heart 2025: Novel Mechanisms of Disease and Arrhythmias
University of Birmingham, UK | 03 – 04 September 2025

C10

L-type calcium channel regulation by β2AR in a coculture model of innervated cardiomyocytes

Jake Burke[1], Sejal Singal[1], Jose L. Sanchez-Alonso[1]

[1]National Heart and Lung Institute, Imperial College London, UK

Introduction. L-Type calcium channels (LTCC) are an essential element in the excitation-contraction coupling of cardiomyocytes (CMs). Recently, we have shown that the regulation of the LTCC activity by proximity coupling mechanisms occurs only via β2AR, but not β1AR, with the requirement of caveolin 3 (Cav3) to form complexes (1). We hypothesise that this mechanism can play a role in tuning the LTCC response by β2ARs under sympathetic stimulation. This study aims to investigates how sympathetic innervation regulates CM adrenergic responses, the effect of innervation on the formation of an LTCC/β2ARs/Cav3 complex(es), and what impact innervation has in driving arrhythmogenic events.

Methods. CMs and sympathetic neurons (SNs) were isolated from neonatal rat pups and cocultured for periods of 3-4 and 7-10 days. Methods ranged from contraction analysis and Ca^{2+} transient with either β1AR or β2AR antagonists by high-throughput multicellular CytoCypher, scanning ion conductance microscopy (SICM), smart patch-clamp, and immunostaining confocal imaging. All experiments were performed under Imperial College London ethical guidelines.

Results. CytoCypher contraction analysis shows how the role of innervation matures over time in culture. At 4 days, innervated CMs show no remarkable differences from non-innervated. However, at 8 days, innervated CMs shows a higher peak of contraction (0.332±SEM, n=19) than non-innervated (0.175±SEM, n=22). Interestingly, using β1AR and β2AR blockers on contracting cells show an overall decrease in time to peak and time to baseline in both innervated and non-innervated, suggesting a competitive role between βAR in our culture conditions. Single channel patch clamp analysis suggest that innervation doubles the open probability of LTCCs (innervated: 0.089, n=4, p=0.0571 vs non-innervated: 0.046, n=4). Through immunostaining of LTCC and Cav3 proteins, we show the presence of LTCC/Cav3 complexes, with a higher co-localisation coefficient on innervated CMs than non-innervated (p=0.0076). Arrhythmia analysis under nicotine stimulation showed that only innervated CMs under β2AR blockage are more susceptible to arrhythmias than any other group tested at both time points (4-day, n=4-5, p=0.0005; and 8-day, n=3-4 p<0.0001 versus control).

Conclusion. Our preliminary results suggest that β2AR plays an important role in the control of CM contraction by sympathetic innervation. Specifically, our results suggest that innervated CMs may have a higher number of LTCC complexes associated with Cav3 and β2AR, and they may be essential in mitigating CM susceptibility to arrhythmias.

C11

Intracellular Ca2+ and circadian rhythms in pro-arrhythmic activity of rat pulmonary vein cardiomyocytes.

Laura MK Pannell[1], Alexander Carpenter[1], Yi Zhe Koh[1], Stephen C. Harmer[1], Hugh D. Piggins[2], Jules C. Hancox[1], Andrew F. James[1]

[1]Bristol Medical School, Faculty of Health & Life Sciences, University of Bristol, UK, [2]School of Psychology & Neuroscience, Faculty of Health & Life Sciences, University of Bristol, UK

Introduction.

Episodes of atrial fibrillation (AF) in patients tend to occur at night. Cardiomyocytes in the pulmonary vein (PV) sleeves are a major source of the ectopic activity driving AF. The pulmonary vein sleeves are highly innervated and it is known that the autonomic nervous system plays a role in the onset of AF. In addition, spontaneous diastolic Ca^{2+} release has been suggested to play a role in the generation of delayed afterdepolarisations (DADs), triggered activity and abnormal automaticity in PV cardiomyocytes.

Aims/objectives.

This study addresses the hypothesis that 24-hr variation in Ca^{2+} release plays a role in circadian rhythms in proarrhythmic activity of PV cardiomyocytes.

Methods.

Animal procedures were approved by the Animal Welfare and Ethics Review Board of the University of Bristol and conducted in accordance with UK law. Male Wistar rats were maintained in a 24-hr cycle of 12-hr light/dark (lights-on at Zeitgeber time, ZT=0; lights-off, ZT12). Hearts were removed under terminal general anaesthesia at 4 times (ZT, Zeitgeber Times) through the 24-hour cycle (ZT 0, 6, 12, 18). Whole-cell current clamp recordings were made from cardiomyocytes isolated from the proximal PV (n=75 cells) and the left atrial appendage (LAA, n=65 cells) of 16 rats and loaded with Cal520-AM (5 μM). The frequency and amplitude of DADs, and diastolic spontaneous Ca release transients (spCaT) were measured and the effects of the cardiac sympathetic neurotransmitter, noradrenaline (NA, 1 μM), examined. DAD and spCaT amplitude and frequency were plotted against ZT of recording and fitted with a sine wave. Fitted curves were compared using an extra-sum-of-squares F-test ($P<0.05$).

Results and Discussion.

Under control conditions, DADs and spCaT could be recorded in both PV and LAA cardiomyocytes, with the frequencies and amplitudes being greatest during the resting phase (ZT0-12) compared to the active phase (ZT12-24) in both cell types. However, DAD/spCaT frequencies and amplitudes were generally greater in PV than in LAA cardiomyocytes in both rest and active phases. Superfusion with NA increased DAD and spCaT frequency and amplitude in both cell types with the greatest effects during the resting phase and in PV cardiomyocytes. DAD amplitude was closely correlated with spCaT amplitude in both

cell types, with the slope of the relation being greater in PV than LAA cardiomyocytes and being increased markedly by NA. There was a ZT-dependence to the slope of the DAD amplitude/spCaT relation under control conditions and in the presence of NA.

Conclusions.

Taken together, these data suggest a role for noradrenergic control of diastolic spontaneous Ca^{2+} release in the circadian rhythms in proarrhythmic activity of PV cardiomyocytes.

Cross-Talk of Cells in the Heart 2025: Novel Mechanisms of Disease and Arrhythmias
University of Birmingham, UK | 03 – 04 September 2025

C12

Neural regulation of cardiac pericytes – a novel mechanism for cardiac regeneration

Nika Barbara Pravica[1], Svetlana Mastitskaya[1], Elisa Avolio[1]

[1]University of Bristol, United Kingdom

Background: Cardiac regeneration after myocardial infarction (MI) critically depends on the restoration of blood flow to the affected area. Angiogenesis, driven by the dynamic interaction between endothelial cells and pericytes, is therefore pivotal for the cardiac recovery after MI. Abundant in the heart's dense capillary network, pericytes regulate vascular tone, modulate immune responses, and play a key role in vessel formation, maturation, and stabilization. Leveraging their regenerative and angiogenic properties offers a promising strategy to ischemic heart repair. Myocardial infarction is associated with autonomic imbalance, characterised by reduced vagal activity. Restoring cholinergic input through vagus nerve stimulation has been shown to exert anti-arrhythmic effects, reduce infarct size, promote angiogenesis, and favour myocardial functional recovery. Despite the recognized importance of neurally derived trophic factors in cardiac regeneration, this aspect remains largely underexplored.

Aim: To explore the potential interplay between autonomic neural regulation and pericytes in cardiac regeneration following MI.

Methods: Human cardiac pericytes are isolated from cardiac surgery waste tissue, expanded in vitro and treated with carbachol (cholinergic agonist) or isoprenaline (b-adrenergic agonist) every 24h at rising concentrations. Cell viability is assessed at 24, 48 and 72h using calcein/EthDIII, while proliferation is evaluated using EdU incorporation after 48h of treatment. To measure cell migration speed and efficiency, wound healing assay is used, and migration is observed during a 24-hour period. Immunocytochemistry is employed to investigate the expression of neurotransmitter receptors. To mimic ischemic conditions in vitro, pericytes are cultured under hypoxia and deprived of growth factors for 24h.

Results: At tested concentrations, neither drug had adverse effects on cardiac pericyte viability or morphology. Preliminary data indicate that neither carbachol nor isoprenaline influences cardiac pericyte proliferation. However, both drugs were found to enhance pericyte migration induced by PDGF-BB. Immunostaining revealed that pericytes express neurotransmitter receptors associated with cardioprotection, including α7 nicotinic and M3 muscarinic acetylcholine receptor.

Conclusion:These findings suggest that autonomic neurotransmitters may enhance pro-angiogenic function of pericytes, supporting the notion that neural modulation contributes to myocardial regeneration. Ongoing studies will further characterize neuroactivated pericytes and downstream signaling pathways involved in vascular repair, guiding future regenerative therapies.

C13

New submission

Rina Sha[1], Olivia Baines[1], Abbie Hayes[1], Sophie Broadway-Stringer[1], Manish Kalla[2], Ming Lei[3], Katja Gehmlich[1], Andrew P Holmes[1], Christopher O'Shea[1], Davor Pavlovic[1]

[1]Univereity of Birmingham, UK, [2]Department of Cardiology, Queen Elizabeth Hospital, Birmingham, UK, [3]University of Oxford, UK

Sodium-glucose cotransporter 2 inhibitors attenuate left atrial electrical remodelling induced by high-fat diet

Rina Sha1, Olivia Baines1, Abbie Hayes1, Sophie Broadway-Stringer1, Manish Kalla1,3, Ming Lei4, Katja Gehmlich1, Andrew P Holmes1,2, Christopher O'Shea1, Davor Pavlovic1

1 Cardiovascular Sciences, University of Birmingham, UK. 2 Institute of Clinical Sciences, University of Birmingham, UK. 3 Department of Cardiology, Queen Elizabeth Hospital, UK. 4 Department of Pharmacology, University of Oxford, UK.

Introduction:

Obesity significantly increases the risk of developing atrial arrhythmias. Sodium-glucose cotransporter 2 (SGLT2) inhibitors, originally used for diabetes management, have shown potential anti-arrhythmic benefits, though their direct effects on atrial cardiac electrophysiology in the setting of obesity are unclear. Our work aims to define the atrial proarrhythmic alterations induced by high-fat diet (HFD) and to test if early treatment with SGLT2 inhibitors can attenuate observed changes.

Methods:

CD1 mice (5–8 weeks old) were randomised into three groups: normal chow, HFD, and HFD + SGLT2 inhibitor. The normal chow group received standard chow and water for 20 weeks. The HFD group were fed HFD and high-fructose (15%) water for 20 weeks. During the last

six weeks, the HFD + SGLT2 inhibitor group received dapagliflozin (3 g/kg/day) in their drinking water. ECGs and echocardiography were performed at weeks 14 and 20. At 20 weeks, blood and urine samples were collected to measure glucose levels. An Olink® Target 48 proteomic cytokine panel was used to assess changes in protein expression of 45 key cytokines in plasma. Left atrial electrical activity was assessed using cardiac optical mapping, measuring action potential duration (APD) and conduction velocity (CV). Effective refractory

periods (ERP) were assessed using an S1-S2 pacing protocol. Optical mapping data analysis was performed with ElectroMap.

Results:

After 20 weeks, the HFD and HFD+SGLT2 inhibitor groups showed significantly greater body weight gain than the normal chow group (28.32 ± 2.66, 25.89 ± 3.45, and 9.43 ± 0.93 g, respectively; $p < 0.0001$). As expected, the HFD + SGLT2 inhibitor group showed glucose in

their urine. No differences were observed in left atrial weight, blood glucose, cytokine biomarkers or ECG parameters. Interestingly, the SGLT2 inhibitor group showed increased left ventricular wall thickness

(Anterior: 1.413 ± 0.0793, 1.525 ± 0.0539, 1.600 ± 0.0781mm, respectively. p>0.05. Posterior: 1.624 ± 0.0861, 1.683 ± 0.0757, 1.952 ± 0.0929mm, respectively. p<0.05). HFD induced substantive pro-arrhythmic changes in the left atria. HFD shortened APD at 30%, 50% and 80% repolarisation (APD30, APD50, APD80), decreased ERP and slowed left atrial CV, compared to the normal chow group. SGLT2 inhibitors attenuated the repolarisation deficits, by increasing APD30, APD50 and APD80 while reducing APD heterogeneities and attenuated the HFD-induced ERP changes (57.60 ± 3.92, 42.40 ± 3.12, 47.40 ± 3.41ms, respectively; p > 0.05).

Conclusions:

HFD induces pro-arrhythmic changes in murine left atria. Interestingly, this occurs in the absence of changes in systemic cytokine/inflammatory markers. SGLT2 inhibitors exhibited substantive anti-arrhythmic effects by modulating cardiac electrophysiology. These findings suggest that early treatment with SGLT2 inhibitors may prevent obesity-induced atrial electrical remodelling. Further studies in obese animal models and patients are warranted to explore their therapeutic role in arrhythmia prevention.

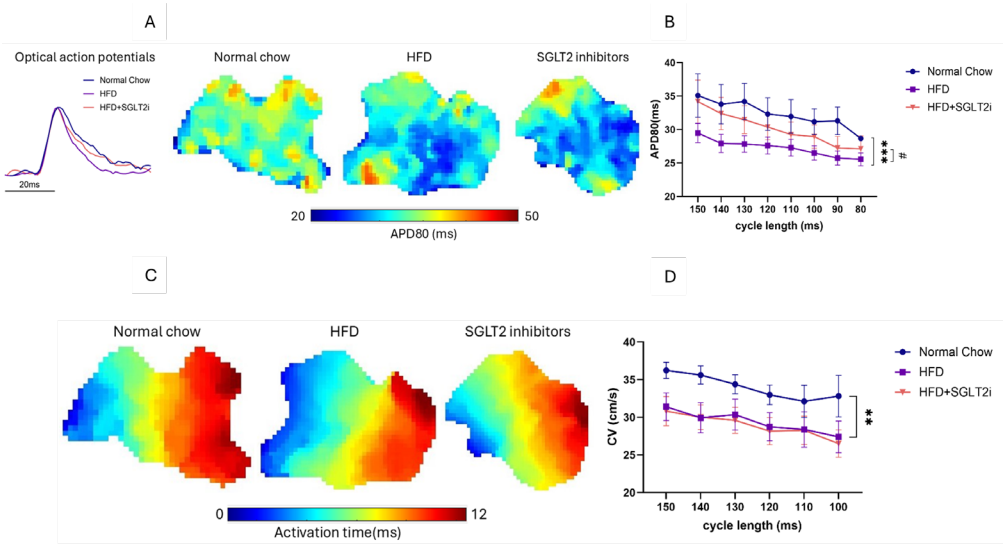

Figure 1: A) Representative action potential duration (APD) 80 map recorded simultaneously from murine left atria of three groups. B) Grouped data of APD 80 in three groups. C) Representative conduction velocity (CV) map recorded simultaneously from murine left atria of three groups. D) Grouped data of CV in three groups. Statistical analysis was conducted using two-way across different cycle lengths. **, *** and # Indicated p < 0.01, p < 0.001and p<0.05 high-fat diet effect and treatment effect at all cycle lengths: n = 6–12.

C14

Correlation of estradiol, progesterone, and estradiol/progesterone ratio with Heart rate variability parameters across menstrual phases in healthy reproductive females.

Darya Abdulateef[1], Tara Salih

[1]University of Sulaimani-College of Medicine, Iraq

Introduction: Heart rate variability (HRV) nowadays is used as an important measure of overall cardiac health and cardiac risk factors. It also relates to better fertility and menstrual regularity in reproductive females, and postmenopausal females are associated with lower heart rate variability compared to reproductive females. There is controversy about the differences in HRV across the menstrual cycle and its correlation with reproductive hormones. The menstrual phase was measured in most studies based on the day of the last menstrual period only, without regard to cycle length.

Objectives: This study aims to compare the HRV parameters between three different phases of the menstrual cycle based on the next cycle and actual cycle length, and to correlate the level of HRV parameters with Estradiol, progesterone, and estradiol/progesterone (E/P) ratio.

Subjects and Methods: In a 103 healthy reproductive female with regular menstrual cycle, after informed consent, participant preparation, and filling questionnaire, HRV parameters were assessed using heart rate sensor and the data for both time domain (RMSSD, SDNN, and mean RR-interval) and frequency domain (LF, HF, and LF/HF) were computed. The blood was received from each participant, and serum Estradiol and progesterone were analyzed. The subjects were divided into three menstrual cycle phases: day 1-11 regarded as phase 1; pre-ovulatory/menstruation phase, 12-18 as phase 2; peri-ovulatory phase, and day 19-28 or till the first day of menses regarded as phase 3; pre-menstrual phase. The actual cycle day for each female was calculated by recording their next cycle from the study time point, and the data were back-extrapolated according to the day of the cycle and cycle length. The hormone levels and levels of HRV parameters between the three phases were assessed using the Kruskal-Wallis test, $P \leq 0.05$. The correlation between parameters was found, and linear regression was used to find significant predictors of HRV parameters, $P \leq 0.05$.

Results: The number of studied participants across menstrual phases is 41, 30, and 32, for phase 1, phase 2, and phase 3, respectively. Compared to other phases, estradiol and HF was significantly higher in peri-ovulatory phase (median HF at phase 1, phase 2 and phase 3: 217.3, 397.26, 243.83 $ms^{2,}$ P=0.036), and progesterone was higher at pre-menstrual phase and E/P ratio at pre-ovulatory phase, other parameters didn't reveal statistically significant differences between menstrual phases. There is a significant correlation between most HRV parameters and estradiol, and the only significant independent negative predictor of HRV (by 19.0%, P = 0.008) and RMSSD (by 12.8%, P = 0.027) is E2 at the premenstrual phase.

Conclusions: There is a significant difference in HRV throughout the menstrual cycle, and HF, which is a measure of parasympathetic function and good overall health of the heart, is highest at the peri-ovulatory phase compared to other phases. The heart rate variability, especially RMSSD, can be used as an independent predictor of estradiol level and reproductive health of females.

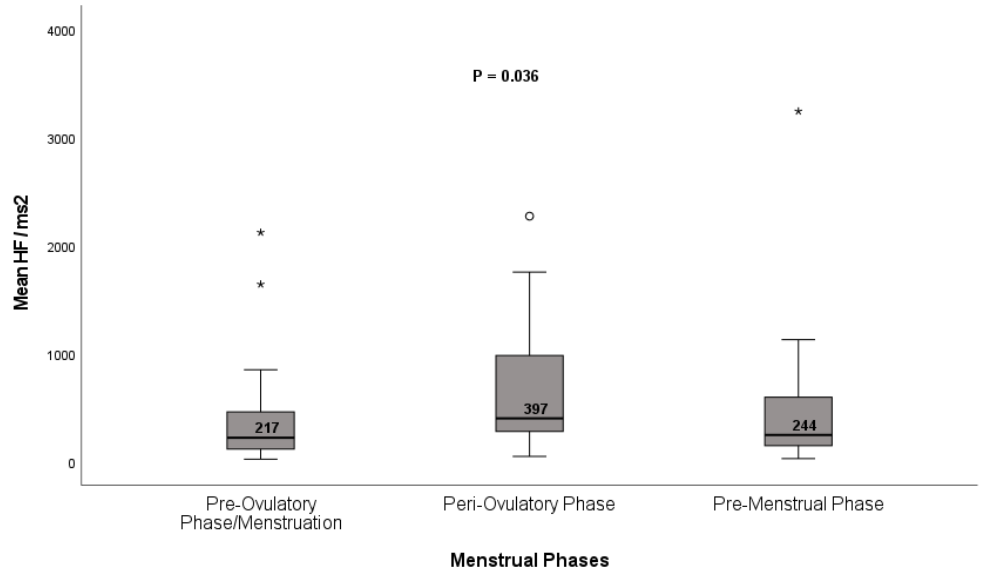

Coefficients[a,b]

Model		Unstandardized Coefficients		Standardized Coefficients		
		B	Std. Error	Beta	t	Sig.
1	(Constant)	39.249	4.703		8.346	<.001
	E2	-.071	.030	-.396	-2.324	.027

a. StagePerActualCycle = Pre-Menstrual Phase

b. Dependent Variable: RMSSD

C15

Understanding the role of LIMP-2 in the lysosomal storage disorder Fabry Disease

Megan Douglas[1], Alex Davies[1], Susan Kimber[1], Karen Piper-Hanley[1], Matthew Birket[1]

[1]University of Manchester, United Kingdom

Fabry disease (FD) is a progressive, X-linked lysosomal storage disorder characterised by globotriaosylceramide (Gb3) accumulation and widespread cellular dysfunction. Although FD affects multiple organ systems, cardiac complications remain the leading cause of patient mortality and current diagnostic methods and therapies remain inadequate. A major barrier to diagnosis and treatment is that the mechanisms of the disease remain poorly understood. Focusing on heart involvement, our lab generated an induced pluripotent stem cell (iPSC) model of FD and identified the lysosomal membrane protein LIMP-2 as a protein which accumulates in FD iPSC-derived cardiomyocytes. Since its functional role in the heart remains unexplored, this study aimed to address this and understand better the disease cascade downstream of Gb3 accumulation. LIMP-2 expression was altered via CRISPR-Cas9 knockout and lentiviral overexpression. LIMP-2 knockout iPSCs were obtained, they remained pluripotent and could be differentiated to cardiomyocytes with high efficiency. Samples were submitted for Gb3 quantification by mass spectrometry and whole cell proteomics ($n = 5$). Early candidate testing identified the gap junction protein Cx43, as significantly increased ($n = 3$, $P < 0.05$) after LIMP-2 overexpression, suggesting Cx43 could be a potential target of LIMP-2. Cx43 has recently been implicated in mediating lysosomal exocytosis under cell stress, hence its upregulation in response to elevated LIMP-2 levels could suggest a cardioprotective mechanism employed to aid Gb3 clearance in FD. Understanding these mechanisms could support the development of better diagnostic methods and therapies for patients with FD and other lysosomal storage disorders.

C16

miR145 as up-stream regulator of vascular senescence and sympathetic innervation in the aging heart

Julian Wagner[1], Clara Bühler[2], Mariano Ruz Jurado[2], Katja Schmitz[2], Josefine Panthel[2], Haris Kujundzic[2], Ariane Fischer[2], Wesley Abplanalp[2], Simone-Franziska Glaser[2], Evelyn Ulrich[2], Tara Procida-Kowalski[3], Marke Bartkuhn[3], Thomas Böttger[4], Stefanie Dimmeler[1]

[1]Goethe-University Frankfurt, Germany, [2]Goethe-Universty Frankfurt, Germany, [3]Justus-Liebig-University Giessen, Germany, [4]Max-Planck-Institute for Heart and Lung Research, Bad Nauheim, Germany

Introduction: Aging is a major risk factor for impaired cardiovascular health. The aging heart is characterized by vascular dysfunction, increased hypertrophy, fibrosis and electrophysiological alterations that predispose the elderly to arrhythmic risk. Previously, we described that aging drives left ventricular (LV) denervation leading to reduced heart rate variability and increased susceptibility to ventricular arrhythmia. Our data demonstrated that aging induces vascular senescence in the LV which impairs the neurovascular interaction leading towards a shift of endothelial axon repelling signals with an increase in the repelling factor Sema3a and decline in the neuroprotective factor Vegfb. However, the mechanisms underlying vascular senescence in the aged heart remain elusive.

Methods: Using micro-array, bulk RNA / snRNA-seq and transgenic mouse models as well as miR-mimics in vivo, we aim to elucidate the molecular mechanisms underlying age-related vascular senescence in the heart. Cardiac remodeling and the innervation are assessed by confocal immunofluorescence imaging.

Results: Micro-array data from 3-month-young versus >18-month-old revealed significant repression of the miR-145-5p. TaqMan-PCR on isolated cardiac endothelial cells (n=4, p=0.0037) and RNA-Scope (n=3, p=0.01) revealed the age-related repression of miR-145-5p specifically in cardiac endothelial cells. Interestingly, miR-145 is known to be predominantly expressed by smooth muscle cells but not in endothelial cells. Global and endothelial-specific miR-143/145-cluster-deletion resulted in pronounced senescence exclusively in arteries (n=4, p<00001). MiR143/145-deletion impaired diastolic function and resulted in left atrial enlargement while the LV mass was unchanged. Anti-miR-145 in vitro experiments in endothelial cells resulted in impaired endothelial migration and proliferation and induced endothelial senescence. SnRNA-seq sequencing confirmed the expression of senescence-associated genes in cardiac endothelial cells in endothelial-specific miR143/145-deletion. Ligand-receptor-predictions revealed that endothelial cells increase the expression of axon-repelling genes such as Sema3a and the up-regulation of matrix protein genes such as collagens and laminins. Indeed, endothelial specific miR143/145-deletion mice showed significantly less sympathetic LV innervation and increased vascular fibrosis. To rescue the age-related decline in miR145 in aged mice, we i.v. injected 1000 pmol of miR-145-mimics to 18-month-old mice which resulted in elevated miR145 levels in the heart. Interestingly, already after 3 days LV innervation tended to be increased while vascular senescence was reduced. A long-term experiment including functional assessments is currently ongoing.

Conclusion: Here, we show that miR145 might be an up-stream regulator of endothelial senescence in the aging heart which contributes to LV denervation in the elderly. Rescuing miR145-levels in the aging heart may restore cardiac innervation and thereby improve heart function.

C17

The effects of cardiac pacing location on ventricular electrophysiology and restitution properties during ventricular fibrillation in the rabbit heart

Bethan Roper-Jones[1], Dr Emily Allen[1], Rachel Sutcliffe[1], Dr Reshma Chauhan[1], Professor G André Ng[1]

[1]University of Leicester, England

Introduction: Ventricular fibrillation (VF) is a malignant arrhythmia associated with Sudden cardiac death (SCD). There is no effective therapies to prevent SCD highlighting the importance of better understanding of VF mechanisms. The electrical restitution property of the heart has been used to determine arrhythmia susceptibility. This is the relationship between Action potential duration (APD) and diastolic interval (DI). Sequential APD changes during VF are believed to still be impacted by preceding APD and DI, referred to as cardiac memory, which could play an important role in VF initiation. Electrical heterogeneity also influences cardiac restitution and arrhythmia susceptibility which can be impacted by pacing location. This study investigates the relationship between APD and DI during VF and the impact of pacing location on restitution, in order to better understand the mechanisms underlying VF initiation.

Methods: New Zealand White Male Rabbits (3-3.5kg) n=8 were sedated via subcutaneous injection (0.2mg/kg Sedator, 10mg/kg Ketamine and 0.01mg/kg Torbugesic). Hearts were isolated for a Langendorff heart preparation. Monophasic Action Potentials (MAPs) were recorded from the apex and base of the left ventricle epicardium. Pacing stimulation protocols such as effective refractory period (ERP), Action potential duration (APD), S1 delay, S2 delay, and standard restitution were conducted from five pacing sites. There were four epicardial pacing sites - Right Ventricle (RV) apex epicardium (epi), RV base epi, left ventricle (LV) apex epi and LV base epi and one endocardial site RV apex. Epicardial Pacing location was randomised. A VF pacing protocol was conducted via pacing at the endocardial site.

Results: There were no significant differences in APD restitution (APDR) max, conduction velocity restitution (CVR) or ERP with pacing at the different locations. However, significant differences were identified in S1and S2 delay when comparing pacing locations. There was a significant difference between LV Apex Epi and RV Base epi for S1 and S2 delay ($p \leq 0.005$) from the Apex MAP recordings. Significant differences were also identified from the Base MAP recordings between LV Base epi and RV Apex epi ($p \leq 0.01$). During VF, a negative relationship was found between APD and preceding DI (up to n-5), but this relationship disappeared after 30 beats (Apex R value = -0.45) with no distinct relationship being found after 90 beats (Apex R value = -0.05). A positive relationship was found between APD and preceding APD (up to x-5) but the similar lack of relationship was found with an average decrease in R value of 0.3.

Conclusions: This study showed that there are no significant differences on electrical restitution when comparing pacing sites except for S1 and S2 delay where there is a distance effect. It was found that there is a relationship within the first 30 beats of VF between APD and DI. These findings highlight the potential of restitution analysis to capture VF dynamics within the first 30 beats of onset. The observation that VF may exhibit non-random, memory-dependent patterns suggests that exploiting this could enable more precise timing of defibrillation and ultimately improve clinical outcomes.

C18

Correlation of alteration of electrical activity and gene expression in the injured zebrafish heart.

Stefania Brown[1], Euan R Brown[2], Gianfranco Matrone[3]

[1]Institute of Neuroscience and Cardiovascular Research, Queen's Medical Research Institute, University of Edinburgh, United Kingdom, [2]School of Engineering and Physical Sciences, Institute of Biological Chemistry, Biophysics and Bioengineering, Heriot-Watt University, Edinburgh, United Kingdom, [3]a Institute of Neuroscience and Cardiovascular Research, Queen's Medical Research Institute, University of Edinburgh, United Kingdom

Background – Zebrafish (Danio rerio), a well-established model of human cardiac disease [1], has the ability to regenerate rapidly after injury [2]. Cardiac recovery after injury is particularly rapid in the larval phase [3]. As zebrafish possesses a similar ventricular action potential and ion channel protein expression to human heart [4], we explored the possibility of using non-invasive electrical recording in the larval stage to measure changes in cardiac electrophysiology along with gene expression during regeneration.

Methods - A PALM MicroBeam laser (Zeiss) was used to produce precise ventricular damage in n=6 transgenic larvae [Tg(myl7:GFP)] at 72 hours post-fertilisation anaesthetized in tricaine (160 mg/L). Cardiac recovery was monitored under tricaine anaesthesia using in vivo electrical extracellular recording at 2 and 24 hours after injury. Cryo-injury, using a cooled copper probe, was used to induce injury in n=6 anaesthetized adult zebrafish hearts, n=6 adults were used as sham. Quantitative PCR (Q-PCR) was used to measure gene expression. For statistics Student's t-tests for paired and unpaired data were used.

Results – Larvae showed regular sequences of wave-forms (a small atrial followed by a larger ventricular depolarization). Larvae (n=6) at 2h post-injury showed one of three states of electrical activity (chaotic small amplitude waves, an atrial depolarisation and no ventricular depolarisation, or an atrial depolarisation and a reduced amplitude ventricular depolarisation). Remarkably, recordings from the same larvae 24h post-injury showed recovery of the normal sequence and amplitude of depolarization ($p<0.05$). Q-PCR analysis in adult hearts showed significant increases in the expression of key ion channel genes in zebrafish at 3 and 7 days post-cryoinjury compared to sham. These genes significantly altered were Scn5lab (ortholog of the human cardiac Na^+ channel; $p<0.001$) [5], KcnK1b (a K^+ two-pore domain K+ channel, expressed in heart that acts upstream of or within heart process; $p<0.0001$), Cacna1ab (a voltage-gated calcium channel subunit alpha Cav2.1; $p<0.01$) and regulatory genes RelA and Tmem161 (highly conserved regulator of cardiac rhythm that function to modulate ion channel activity in zebrafish; $p<0.001$) [6].

Conclusions - We characterised, for the first time, the changes of the electric phenotype in zebrafish larval hearts following injury. This electrical phenotype is highly reproducible and could be mediated by changes in the expression of membrane ion channel genes, as it was observed in the adult injured zebrafish heart.

Ethical standards - Zebrafish used in this study were maintained in the zebrafish facility of the University of Edinburgh according to standard procedures and ethical guidelines.

C19

Functional nanoimaging of neuro-cardiac junctions

Sejal Singal[1], Jake Burke[1], Julia Gorelik[1], Jose L. Sanchez-Alonso[1]

[1]Imperial College London, United Kingdom

Introduction: Abnormal activity of sympathetic neurons (SN) drives cardiomyocytes (CM) to a diseased state. Therefore, it is important to understand how the SN forms contact with CM in the neuro-cardiac junction (NCJ). However, which structural proteins maintain adhesion between two cell types in NCJ is unknown. Voltage-gated sodium channel (Nav1.5) has been observed to maintain adhesion between two CMs in the intercalated discs. Nav1.5 is trafficked to the surface of the CM membrane by an adaptor protein, Ankyrin-G (AnkG). So, the involvement of Nav1.5 in maintaining NCJ adhesion is investigated in this study by interrupting the interaction between Nav1.5 and AnkG with a blocking peptide.

Methods: Ventricular CMs and SNs from neonatal rat pups are cocultured together for 2-5 days or 7-10 days. Experiments were performed under Imperial College ethical guidelines. Single channel scanning ion conductance microscopy (SICM) patch-clamp was used to record sodium current in different regions of innervated CMs. Different regions include on the NCJ, near NCJ (0.1-2μm) and far from NCJ (2.5-12μm). Immunostaining with super resolution confocal imaging was used to visualise the distribution of Nav1.5 and AnkG in innervated and non-innervated CMs.

Results: The results showed that in the first 2-5 days of culture, Nav1.5 is evenly spread throughout the different regions of innervated CMs (n=7-22). Prolonged innervation with 7-10 days culture promoted redistribution of Nav1.5 in CM membrane with a preference in the NCJ region of (2.7±1.0pA) versus the lack of Nav1.5 in areas near the NCJ region (0.6±0.2pA; $p=0.0025$). Immunostaining also showed a similar distribution of Nav1.5 and AnkG, with the highest intensity being found in the NCJ region and the least near the NCJ region (N=3-4 replicates; n=14-16 cells). The colocalisation showed a positive correlation for the distribution of Nav1.5 and AnkG traces in both 2-5 days ($r=0.7217$, $p<0.0001$) and 7-10 days ($r=0.5372$, $p<0.0001$).

Conclusion: Collectively, the results show that innervation promotes the redistribution of Nav1.5 in innervated CM membranes, possibly by an AnkG-dependent mechanism.

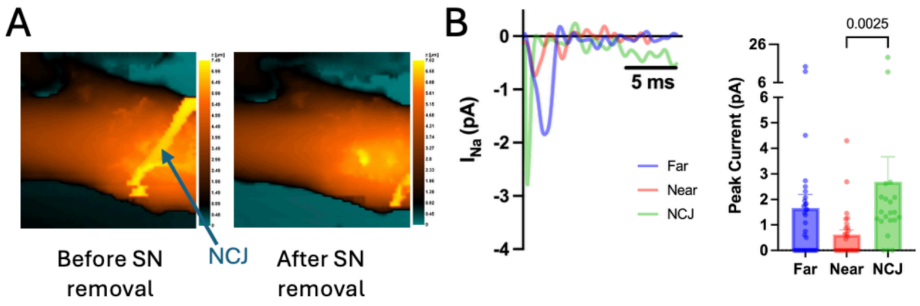

Figure 1. Differences in the peak sodium current in different regions of innervated neonatal rat ventricular cardiomyocytes cultured for 7-10 days. A. Representative scans for innervated cardiomyocyte (CM) before and after removal of sympathetic neuron (SN) present above the CM to record the sodium current of neuro-cardiac junction (NCJ). **B.** Representative traces for recordings and quantification of peak sodium current (I_{Na}) in different areas of innervated CM (far, near or NCJ; n=21-34). Differences are tested using Kruskal-Wallis test with Dunn's post-hoc. Data is represented as mean ± SEM and their distribution is shown with individual dots.

C20

Inflammatory response in a clinically relevant progressive model of chronic kidney disease-associated cardiomyopathy

Katie tompkins[1], Abbie Hayes[1], Katie Bruce[1], Michael Sagmeister[1], Rowan Hardy[1], Andre Ng[2], Davor Pavlovic[1], Christopher O'Shea[3]

[1]University of Birmingham, United Kingdom, [2]University of Leicester, United Kingdom, [3]University of Warwick and University of Birmingham, United Kingdom

Introduction

Chronic kidney disease (CKD) affects 10-15% of the global population. CKD causes systemic inflammation (marked by elevated levels of C-reactive protein, interleukins and tumour necrosis factor-alpha) and CKD-associated cardiomyopathy characterised by increased left ventricular mass, diastolic and systolic dysfunction, profound cardiac fibrosis and atrial and ventricular arrhythmias. The mechanistic links between CKD induced systemic inflammation and cardiac remodelling are unclear, especially in early CKD stages.

Therefore, we aim to characterize a CKD mouse model using an adenine-rich diet to compare structural and functional changes in CKD-related cardiomyopathy between early and late stages, and the link to cardiac electrophysiological alterations and other systemic consequences from CKD.

Methods

8–9-week-old C57BL/6 female and male mice were fed a normal chow or 0.15% adenine rich diet, for up to 7-weeks. Following the diet, blood levels of creatinine and urea were measured to assess kidney dysfunction. Optical mapping was conducted to assess the cardiac electrical activity, comparing adenine-fed mice to control.

Results.

Significant and progressive increase in urea (5-week, $p = 0.0053$ and 7-week, $p < 0.0001$) and creatinine (5-week, $p = 0.0017$ and 7-week, $p < 0.0001$) levels were observed between control and adenine-fed mice, reflecting kidney dysfunction, see figure 1. Optical mapping analysis identified adenine-induced CKD prolongs action potential duration, as seen in figure 2.

Conclusion

The adenine-rich diet induced progressive CKD in this mouse model, which is associated with significant systemic inflammation and early cardiac remodelling characterised by increased fibrosis. Furthermore, adenine-diet induces electrophysiological alterations by prolonging action potential duration.

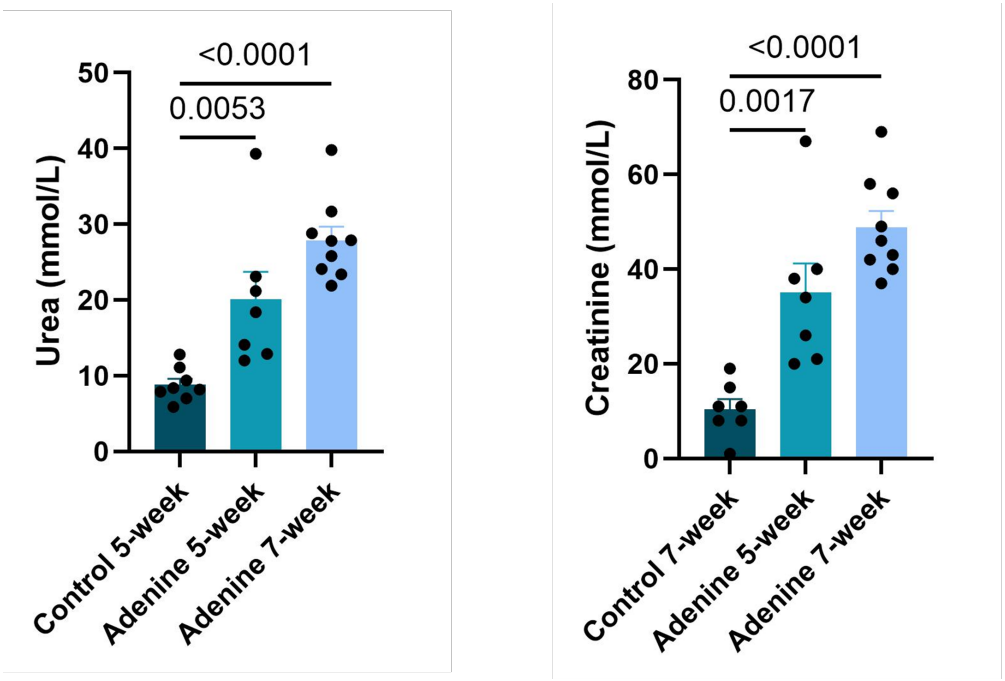

***Figure 1**.) Indicators of kidney damage in adenine-fed mice. A.) Urea levels from normal chow 7-weeks, and adenine-fed mice at 5 and 7-weeks. 1-way ANOVA test results represented by significant values (p=0.0053 and p<0.0001). B.) Creatinine levels from normal chow 7-weeks, and adenine-fed mice at 5 and 7-weeks. 1-way ANOVA test results represented by significant values (p=0.0017 and p <0.0001).*

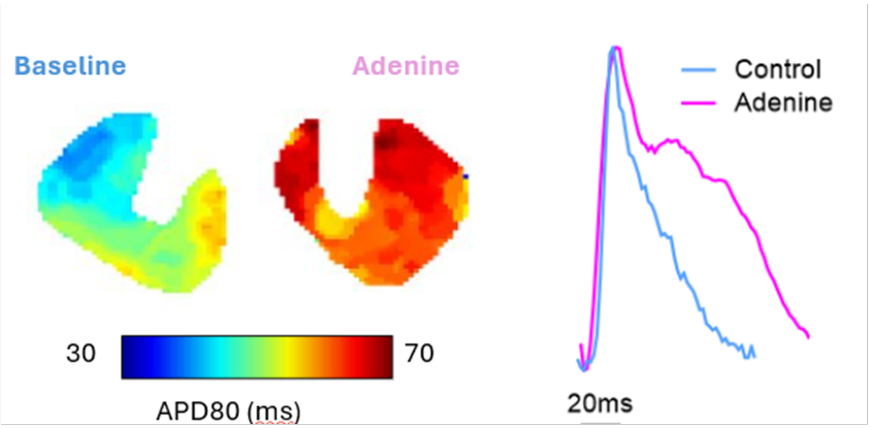

Figure 2.) (A) *Maps identifying the APD prolongation at APD80. (B) Alongside and example action potential, showing the prolongation in the adenine-fed group: pink = adenine prolonged, blue = control.*

C21

Precision ultra-hypofractionated radiotherapy to the stellate ganglia for ventricular arrhythmia (the first in man RADIO-STAR trial)

Benjamin Bussmann[1], Ben George[2], Maxwell Robinson Robinson[3], Tom Whyntie[2], Prabakar Sukumar[3], Ebison Chinherende[2], Fintan Sheerin[3], Veni Enzhil[2], Ami Sabharwal[3], Neil Herring[4]

[1]University of Oxford, united kingdom, [2]Genesis Care, Oxford, United Kingdom, [3]Oxford University Hospitals NHS Foundation Trust , United Kingdom, [4]University of Oxford, United Kingdom

Introduction

Sympathetic activation is a hallmark of cardiac disease, contributing to disease progression and triggering ventricular arrythmias (VA)[1]. While implantable cardioverted defibrillators (ICD) improve mortality by terminating VAs, many patients experience recurrent ICD therapies, leading to worse outcomes and quality of life[2]. Cardiac sympathetic denervation (CSD) through surgical removal of the stellate ganglia has emerged as an effective treatment for refractory VAs[3] but carries a complication rate of up to 50%[3,4]. Direct cardiac radiotherapy to treat refractory VA has also been shown to be both safe and effective[5], but whether radiotherapy can be targeted at the stellate ganglia is unknown. We therefore hypothesised that high precision image guided radiotherapy can be used to target the stellate ganglia to achieve CSD non-invasively leading to fewer complications while still maintaining efficacy.

Methods

RADIO-STAR (ISRCTN 49861434, REC/SC/0005) is a phase 1 clinical trial to determine the feasibility and safety of non-invasive CSD achieved through image guided radiotherapy to the stellate ganglia. 13 patients with structural heart disease who experience recurrent ICD therapy during the preceding 6 months despite optimum medical therapy are invited to undergo image guided radiotherapy bilaterally to the lower half of the stellate ganglia and T1-2 sympathetic chain. A baseline 1.5T MRI of the stellate ganglia is used to determine feasibility of delivering radiotherapy to the stellate ganglia within dose constrains of nearby organs at risk and ICD devices. Radiotherapy is then delivered over 3 fractions on alternate days with total dose escalating from 24 to 33 Gy according to a dose escalation protocol. Participants are followed up for 6 months including continuous ICD device monitoring and repeat stellate ganglion MRI. Safety (adjourned by an independent safety committee) is the primary outcome, and the study is powered ($\beta = 80\%$, $\alpha = 0.05$) to detect a serious adverse event rate of 34%. Secondary outcome measures to evaluate efficacy include radiotherapy induced changes in circulating catecholamine and neuropeptide-Y levels, ICD therapy burden, heart rate variability (HRV) and structural changes in the stellate ganglia on MRI imaging.

Results

We have developed MRI protocols that allow clear visualisation of the stellate ganglia, while limiting ICD related image artefacts (Figure 1A-C). In all 5 patients that so far have undergone baseline MRI it was possible to clearly visualise the stellate ganglia and plan for radiotherapy within dose constraints of nearby organs at risk. To date, three patients have completed radiotherapy treatment (24 Gy), without

serious adverse events. All patients remain arrhythmia free following treatment, with improved autonomic balance on HRV measurements (Figure 1D-F).

Conclusion

We have developed a protocol for targeting the stellate ganglia with radiotherapy to achieve non-invasive CSD. Preliminary findings indicate that this approach is feasible and appears safe; however, further patient recruitment is needed to confirm safety and evaluate efficacy.

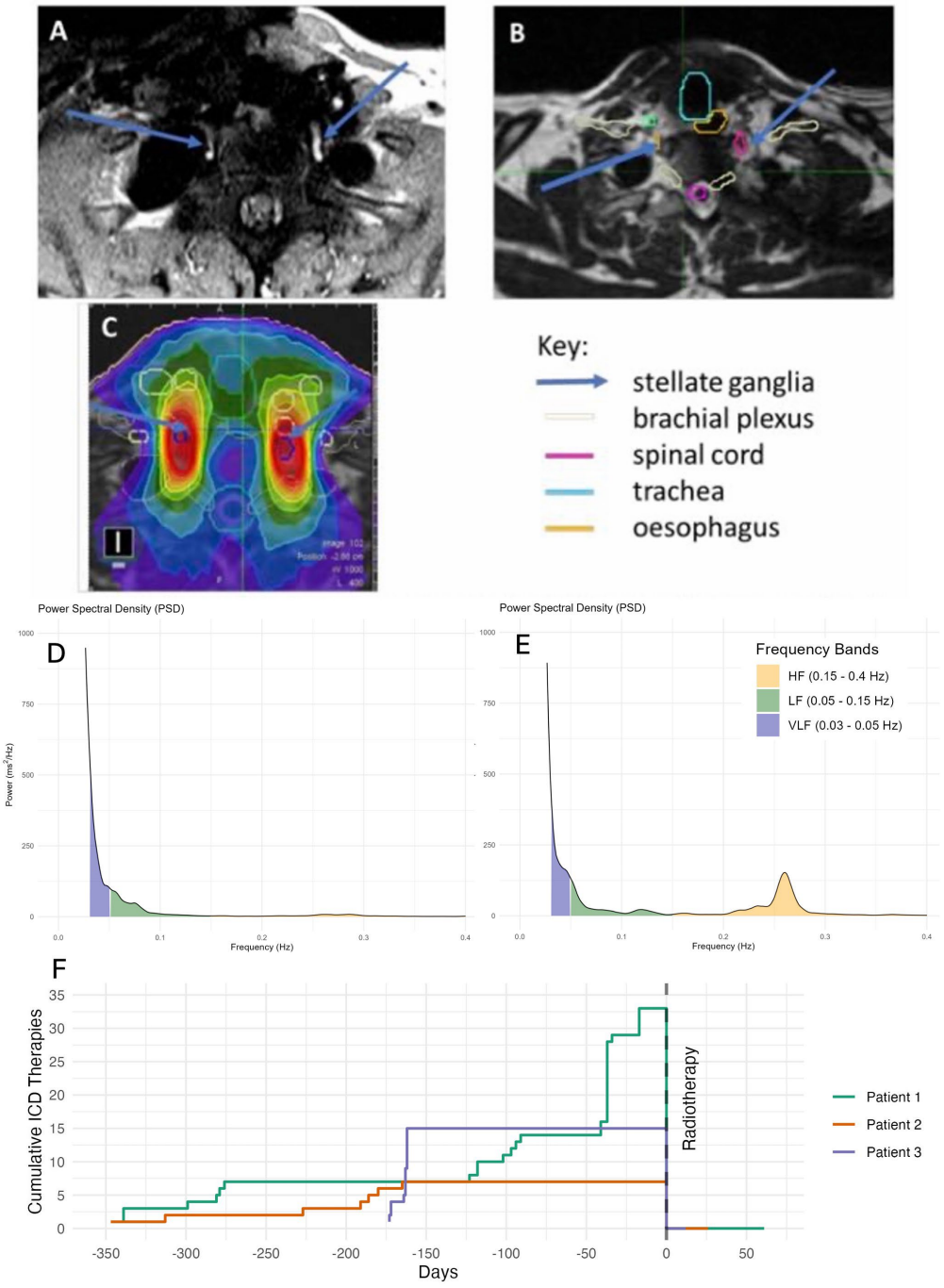

Figure 1: T2 weighted short tau inverted recovery (STIR) MRI of a participant with a left sided transvenous ICD device, demonstrating the stellate ganglia (blue arrows). B) treatment planning contours of the stellate ganglia and nearby organs of risk. C) Radiotherapy treatment isodoses, with high doses (red) over the stellate ganglia and rapid drop of over nearby structures. Power Spectral Density plots before (D) and after (E) completion of radiotherapy to the stellate ganglia show an increase in power of the high frequency band and mild decrease in the low frequency bad, suggesting improved autonomic balance. (F): A step plot showing ICD therapy burden before and after radiotherapy.

C22

Expression and release of bone morphogenetic protein 10 from cardiomyocytes in the adult heart and its regulation by PITX2 enhancer.

Julius Ridder[1], Laura C Sommerfeld[1], Muhammed I Sönmez[1], Alexander Froese[2], Thomas de Saint Nicolas[3], Gemma Sanguesa[3], Jasmeet Reyat[4], Katja Gehmlich[5], Davor Pavlovic[5], Christopher O'Shea[6], Vaishnavi A Murukutla[1], Justus Stenzig[7], Friederike Cuello[7], Paulus Kirchhof[8], Hermann Reichenspurner[9], Viacheslav Nikolaev[2], Torsten Christ[7], Cristina E Molina[10], Larissa Fabritz[1]

[1]University Center of Cardiovascular Science UCCS, University Medical Center Hamburg-Eppendorf, Martinistr. 52, 20246 Hamburg, Germany, [2]Department of Experimental Cardiovascular Research, University Medical Center Hamburg-Eppendorf, Martinistr. 52, 20246 Hamburg, Germany, [3]Institute of Cardiovascular Sciences, University of Birmingham, B15 2TT Birmingham, United Kingdom, [4]Institute of Cardiovascular Sciences, University of Birmingham, B15 2TT Birmingham, United Kingdom , [5]Department of Cardiovascular Sciences, Univeristy of Birmingham, Birmingham B15 2TT, United Kingdom, [6]Department of Cardiovascular Sciences, Univeristy of Birmingham, Birmingham B15 2TT and Division of Biomedical Sciences, Warwick Medical School, Clinical Sciences Research Laboratory, Coventry., United Kingdom, [7]Department of Experimental Pharmacology and Toxicology, University Medical Center Hamburg-Eppendorf, Martinistr. 52, 20246 Hamburg, Germany, [8]University Heart and Vascular Center Hamburg, Department of Cardiology, Martinistr. 52, 20246 Hamburg, Germany, [9]University Heart and Vascular Center Hamburg, Department of Cardiovascular Surgery, Martinistr. 52, 20246 Hamburg, Germany , [10]Department of Experimental Cardiovascular Research and UCCS, University Medical Center Hamburg-Eppendorf, Martinistr. 52, 20246 Hamburg, Germany

Background:

Atrial fibrillation (AF), the most prevalent sustained arrhythmia, is strongly associated with genetic variants near the PITX2 locus on chromosome 4q25. Recent studies suggest an inverse regulatory relationship between PITX2 and bone morphogenetic protein 10 (BMP10), a developmental factor increasingly recognized as a potential circulating biomarker for AF. However, mechanistic data linking PITX2 regulation to BMP10 release levels and its impact on cardiac electrophysiology remain limited.

Purpose:

We aimed to quantify cardiac BMP10 mRNA and protein in adult human heart chambers and determine baseline cardiac BMP10 release from isolated primary human cardiomyocytes. Further we set to quantify Pitx2 expression across cardiac chambers of wildtype (WT), heterozygous (HET), and homozygous (HOM) mice with a Pitx2 enhancer deletion and detect chamber-specific Bmp10 protein release in those groups. Finally we wanted to characterize electrophysiological differences in left atria (LA) of mice with a Pitx2 enhancer deletion, including their response to sodium channel blockade by flecainide.

Methods:

We used discarded atrial tissues from cardiac surgery—primarily small samples from appendages of both atria—to quantify BMP10 gene and protein concentrations in the human heart. mRNA was quantified by RT-PCR. BMP10 protein concentrations in cardiac chamber lysates and culture supernatants of isolated primary human cardiomyocytes were quantified by ELISA. Murine Pitx2c expression was quantified via RT-PCR (n=6). LA, RA, and ventricular tissues from Pitx2 enhancer deletion mouse model were cultured ex vivo, to assess Bmp10 release in supernatant using ELISA (n=12).

Electrophysiological properties of isolated murine LA (n=12) were evaluated via sharp microelectrode recordings at multiple pacing cycle lengths, at baseline and after 1 µM flecainide perfusion.

Results:

In human cardiac chambers RA tissue showed highest BMP10 expression on gene and protein level. Compared to LA protein expression BMP10 was ~240-fold higher in RA. Culture supernatants of primary human cardiomyocytes isolated from the RA had highest BMP10 amount compared to other chambers. LA Pitx2c expression was significantly reduced in mice with a homozygous Pitx2 enhancer deletion to 1/3 of WT levels (Fig 1). RA tissue released detectable Bmp10 ex vivo, with HOM RA showing the highest release (0.383 ± 0.04 ng/mg) (Fig 2). LA electrophysiology showed genotype-dependent changes in resting membrane potential, upstroke velocity (Vmax), and action potential duration (APD90).

Conclusions:

This study establishes the adult human and murine RA as the predominant cardiac source of BMP10 synthesis and release. Further it shows that reduced Pitx2 expression via enhancer deletion is associated with increased Bmp10 release and LA electrophysiological remodelling.

Novelty:

This study provides the first quantitative evidence of BMP10 in both -expression and release- in human and murine heart tissue and cardiomyocytes. We demonstrate that reduced Pitx2 expression in the LA is associated with increased Bmp10 release from the right atrium. In a mouse model with a Pitx2 enhancer deletion, we establish a link between the enhancer deletion, left atrial Pitx2 expression and altered electrophysiological properties. These findings support a functional link between Pitx2 and Bmp10 in atrial pathophysiology, relevant to atrial fibrillation and potential biomarkers of atrial fibrillation.

Fig 1

Pitx2c tissue expression

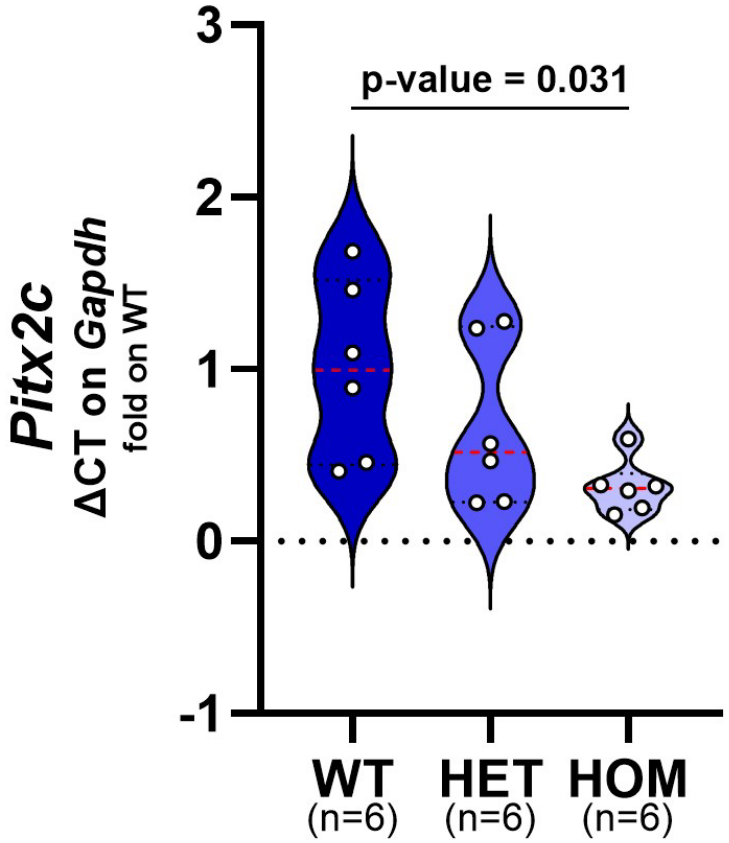

Murine LA
PITX2 Enh. Del. model

Fig 2

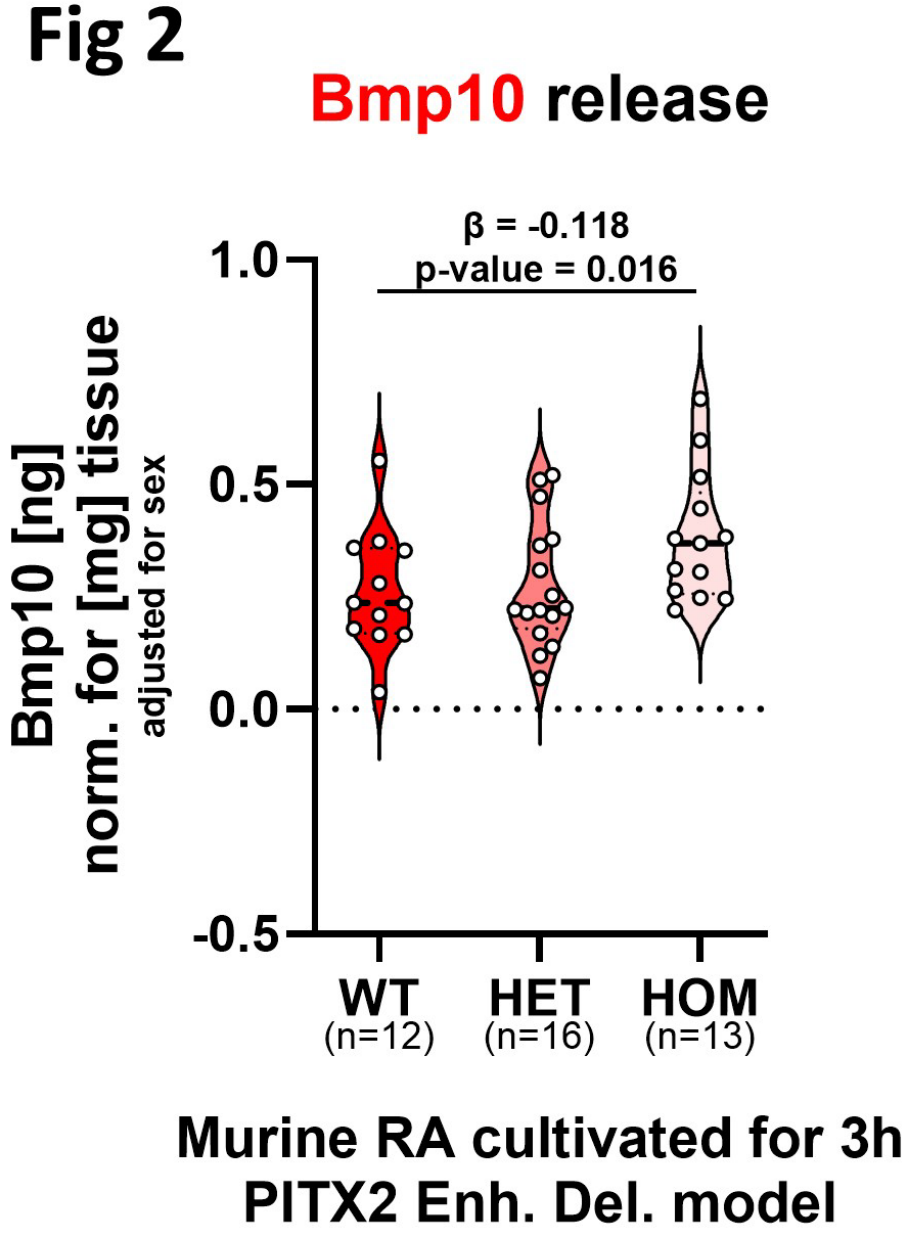
Bmp10 release
β = -0.118
p-value = 0.016
Bmp10 [ng]
norm. for [mg] tissue
adjusted for sex
1.0
0.5
0.0
-0.5
WT
(n=12)
HET
(n=16)
HOM
(n=13)
Murine RA cultivated for 3h
PITX2 Enh. Del. model

Cross-Talk of Cells in the Heart 2025: Novel Mechanisms of Disease and Arrhythmias
University of Birmingham, UK | 03 – 04 September 2025

C23

Evaluation of the importance of Ca2+ binding to fluorescent probes for measurement of the time course of Ca2+ transients in cardiac ventricular muscle.

Daniel Aston[1], Jianshu Hu[1], Charalampos Sigalas[1], Derek Terrar[1]

[1]University of Oxford, UK

Accurate measurements of the time course of Ca^{2+} transients (CaTs) during cardiac action potentials are essential for our understanding of the underlying physiology. This is particularly important for evaluation of Ca^{2+} flux balance across the surface and intracellular membranes. Fluorescent probes for Ca^{2+} have been crucial for the measurement of CaTs. However, all experimental methods have their limitations and the kinetics of Ca^{2+} binding to the probe will inevitably influence the time course of the measured CaT. Greater Ca^{2+} binding would be expected to slow the signal. The dissociation equilibrium constant (Kd) for Ca^{2+} binding to the probe gives some indication of the extent of this disturbance (although the magnitude of forward and backward rate constants for binding will be important as well as their ratio), and stronger binding of Ca^{2+} is expected to cause greater slowing of CaT time course. The commonly used Fura-2 shows strong Ca^{2+} binding with a Kd of approximately 0.14 μM. CaTs measured with Fura-2 show very little decline during the action potential plateau (e.g. Banyasz et al, 2012). Fluo-3 (Kd = 0.39 μM) gives a slighter faster time course though still slow, while Fluo-5F (Kd 2.3 μM) gave CaTs with a more rapid rapid upstroke and decay (e.g. Capel et al, 2015). Rhod-2 (Kd = 0.57 μM) gave rapid upstroke and decay both in isolated myocytes (Fenandez-Tenorio & Niggli, 2016) and whole hearts (Nemec et al 2010).

The experiments presented here were in whole hearts and isolated myocytes. CaTs were measured in ventricular muscle in Langendorff-perfused guinea-pig hearts under conditions similar to those previously published (Nemec et al 2010; Lee et al 2012). Rhod-2 gave a CaT with a peak at around 25 ms (24.6 ± 4.1 ms, n=3) at body temperature, recorded from the left ventricle. This is similar to that measured in previous experiments in Langendorff hearts (Lee et al, 2012, Nemec et al 2010), and also in isolated ventricular myocytes (Fenandez-Tenorio & Niggli, 2016). It might be thought that Rhod-FF with a Kd of 19 μM would give a negligibly small signal, but this was not the case and CaTs were measurable with a peak at approximately 10 ms (10.0 ± 0.9 ms, n=4, significantly different from Rhod-2, $P<0.05$, two sample t-test). CaTs and Ca^{2+} sparks were also recorded using Rhod-FF in mouse isolated ventricular myocytes.

The above observations underline the importance of the kinetics of Ca^{2+} binding to the fluorescent probe for the measurement of the time course of CaTs. The necessity of Ca^{2+} binding to any Ca^{2+} probe will inevitably slow CaTs, but the measurements with Rhod-FF show that the time to peak can be as little as 10 ms, and the time course of CaTs is expected to be even faster in the absence of a Ca^{2+}-binding fluorescent probe.

Cross-Talk of Cells in the Heart 2025: Novel Mechanisms of Disease and Arrhythmias
University of Birmingham, UK | 03 – 04 September 2025

C24

Exploring the autonomic control of ventricular tachyarrhythmias

Danila Fedotov[1], Raimondo Ascione[1], Svetlana Mastitskaya[1], Andrew James[1]

[1]University of Bristol, United Kingdom

One of the most common causes of pre-hospital mortality in patients with myocardial infarction is the onset of ventricular arrhythmias (VAs). Despite the advances in the understanding of underlying molecular mechanisms of VAs, the search for novel preventive treatment of VAs remains a priority. The impact of parasympathetic control to the prevention of VAs provided by the vagus nerve through the parasympathetic ganglia remains insufficiently studied. It has been previously demonstrated that glucagon-like peptide-1 receptors (GLP-1R) are located on both vagal post-ganglionic neurones and ventricular cardiomyocytes. Moreover, their activation using the GLP-1R agonist, Exendin-4, resulted in prolonged effective refractory period (ERP) and, thereby, reduced arrhythmia inducibility (Ang et al., 2018). This antiarrhythmic effect is mediated through muscarinic receptors and nitric oxide (NO), suggesting a complex interaction between GLP-1R signalling and classical parasympathetic neurotransmitters, including acetylcholine, NO, and vasoactive intestinal peptide (VIP).

To assess the left ventricular electrophysiological responses to sympathetic and parasympathetic agonists we used a mouse isolated Langendorff perfused heart model. For stimulation we used S1-S2 protocol at cycle lengths (CL) of 40 ms, 60 ms, 80 ms, 120 ms, 160 ms. Interestingly, no rate-dependent shortening of ERP was observed. Mean (±SD) values for ERP were therefore calculated over all the CLs measured. The mean ERP in control group (n=10) was 35.0±11.4 ms, was significantly prolonged by carbachol (n=7, 1 μM: ERP 40.8±11.2 ms; $p<0.05$), and shortened by isoprenaline (ISO, 1 μM, n=8, ERP 28.4±5.0 ms; $p<0.05$). We hypothesised that the opening of KATP channels contributed to the ERP shortening upon sympathetic stimulation (Kim et al., 2012). The effects of ISO on ERP were completely abolished in the presence of KATP channel blocker glibenclamide (n=5, 10 μM, ERP 36.7±12.3 ms; $p=0.437$), indicating potential antiarrhythmic properties of this antidiabetic drug. We will examine the involvement of KATP channels in the effects of GLP-1R activation. Further research on the modulation of VT/VF susceptibility by GLP-1R agonists and downstream signalling mechanisms in normoxic and ischaemic conditions could ultimately lead to the development of new therapeutic approaches for the treatment and prevention of ventricular tachyarrhythmias.

Cross-Talk of Cells in the Heart 2025: Novel Mechanisms of Disease and Arrhythmias
University of Birmingham, UK | 03 – 04 September 2025

C25

Weight Loss Reverses Left Atrial Electrical Remodelling Associated with Obesity in Mice Fed High Fat Diet

Olivia Baines[1], Rina Sha[1], Tanvi Raut[1], Sophie Broadway-Stringer[1], Abbie Hayes[1], Katja Gehmlich[1], Manish Kalla[1], Andrew P Holmes[1]

[1]University of Birmingham, United Kingdom

Introduction: Obesity affects 1 in 8 people globally and has been independently associated with arrhythmia incidence, including atrial fibrillation (AF). Standard anti-arrhythmic therapies have shown poorer response rates in obese patients. Weight loss has been shown to improve AF outcomes. However, the mechanisms underlying obesity-mediated pro-arrhythmia and the therapeutic effects of weight loss remain unclear. This study aimed to determine whether weight loss reverses obesity-induced left atrial pro-arrhythmic remodelling in mice fed a high-fat diet (HFD).

Methods: Male and female CD1 mice (5-8 weeks old) were assigned to three groups: 1) control (normal chow and water for 20 weeks), 2) HFD (60 kcal% fat) with 15% fructose water for 20 weeks, or 3) weight loss (HFD and fructose water for 14 weeks, followed by normal chow and water for 6 weeks). In vivo echocardiography, ECG, ex vivo left atrial optical mapping and O-link plasma proteomics were performed at 19 to 20 weeks.

Results: HFD mice demonstrated significantly higher body weight (61.9 ±7.24g versus 40.8 ± 5.75g, $p<0.0001$) and blood glucose (18.3 ± 3.19 mMol/L versus 14.9 ± 2.34 mMol/L, $p<0.05$) versus control. The weight loss group achieved significant body weight reduction compared to HFD (45.5 ± 9.78g versus 61.9 ±7.24g, $p<0.01$). Systolic, diastolic and myocardial strain parameters were unchanged across all groups. HFD mice also showed similar heart chamber dimensions to control. ECG characteristics were also similar between groups, except for reduced R wave amplitude in HFD and weight loss mice versus controls (control: 0.601± 0.0591mV, HFD: 0.416±0.0457mV ($p=0.0644$), weight loss: 0.379 ±0.0495mV ($p<0.05$)). Optical mapping revealed shortened left atrial action potential duration at 30, 50 and 80% (APD30, APD50, APD80) repolarisation for HFD mice, compared to control (Figure 1, A-B). Weight loss attenuated APD prolongation and reduced APD80 spatial heterogeneity (Figure 1, A-C). Left atrial effective refractory period (ERP) showed a similar trend, although non-significant, where HFD mice displayed a shorter ERP than control (42.4 ± 6.99 ms vs 57.6 ± 8.76 ms). Weight loss partially recovered the ERP (46.0 ± 11.6 ms). Plasma proteomics demonstrated no significant alteration in overall systemic inflammation between groups (Figure 2, A). However, CCL11 and CCL5, markers linked to myocardial fibrosis and heart failure, were significantly reduced in weight loss mice compared to control.

Conclusions:

20-week HFD induced significant left atrial pro-arrhythmic remodelling, with preserved systolic and diastolic function. Notably, HFD-associated pro-arrhythmic changes occurred in the absence of systemic inflammation. Weight loss ameliorated HFD-induced atrial electrical remodelling, further supporting weight management as a strategy for mitigating obesity-related AF risk.

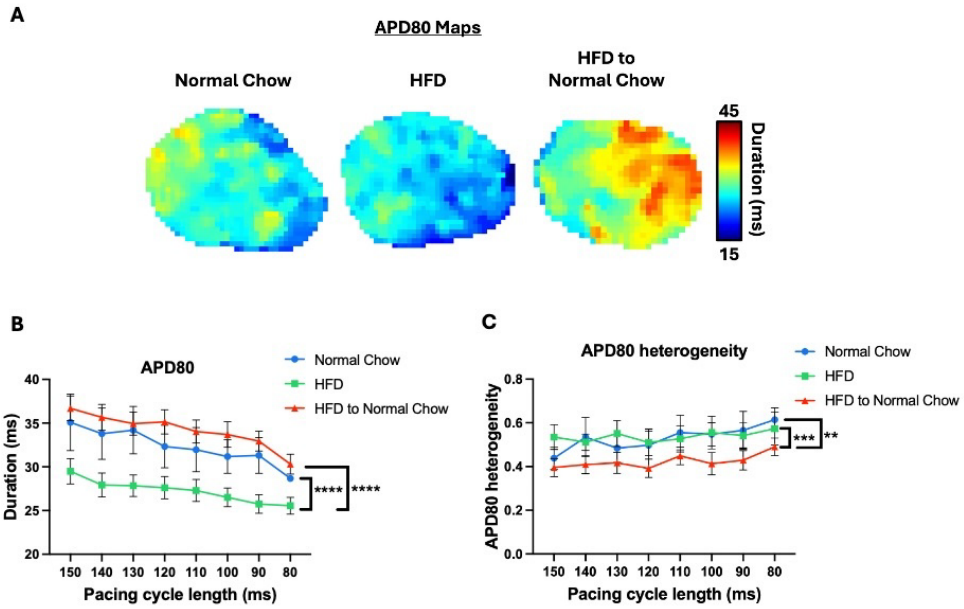

Figure 1. Left atria ex vivo optical mapping at 20 weeks. *(A) Representative action potential duration at 80% repolarisation (APD80) maps. (B) APD80 and (C) APD80 heterogeneity restitution curves. Data presented as mean ± SD or SEM. '*'; p<0.05, '**'; p<0.01, '***'; p<0.001, '****'; p<0.0001 analysed by one-way ANOVA or two-way ANOVA followed by Tukey's post-hoc test. HFD= high-fat diet.*

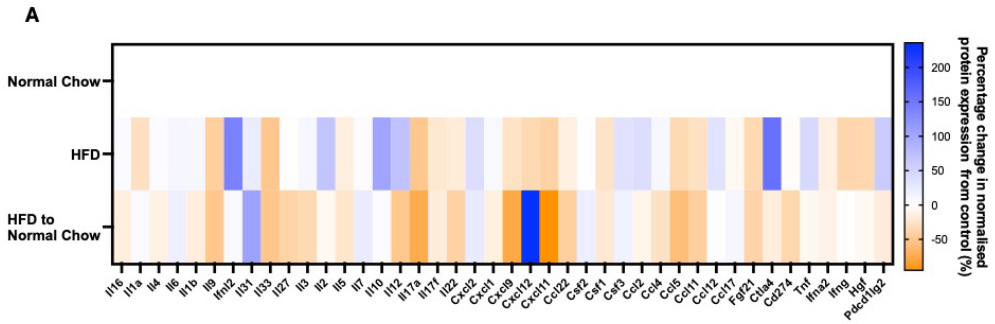

Figure 2. Plasma proteomics at 20 weeks. *(A) Heat map demonstrating mean percentage change in normalised protein expression compared to control, illustrated by adjacent isochronal scale. Data presented as mean ± SD. '**'; p<0.01 analysed by one-way ANOVA followed by Tukey's post-hoc test. HFD= high-fat diet*

Cross-Talk of Cells in the Heart 2025: Novel Mechanisms of Disease and Arrhythmias
University of Birmingham, UK | 03 – 04 September 2025

C26

Targeted genetic catecholaminergic ablation in cardiomyocytes disrupts atrioventricular conduction stability during post-provocative pacing

Shea-sarah Garcia, Tianyi Sun, Ming Lei

[1]University of Oxford, UK

Introduction

While extrinsic autonomic input regulates atrioventricular (AV) conduction, the functional role of intrinsic non-neuronal catecholaminergic sources is incompletely understood. Dopamine β-hydroxylase-expressing cardiomyocytes (Dbh-CMs) were abundantly identified within the AV node however, their contribution to nodal excitability remains untested (Sun et al., 2023). Here, we use a tamoxifen (TAM)-inducible cardiomyocyte-specific Dbh conditional knockout line (Dbh-cKO) to bypass developmental compensation and assess whether intrinsic Dbh-CMs influence AV nodal conduction in the adult heart—bridging structural discovery with functional insight.

Aims

To functionally characterise intrinsic catecholaminergic cardiomyocyte influence on AV nodal conduction reserve.

Methodology

Dbh-cKO mice (C57BL/6J mixed-sex) were generated by crossing $Dbh^{+/Flox}$ mice with MHC-CreERT2 ($A1cf^{Tg(Myh6\text{-}cre/Esr1*)1Jmk}$) mice. Four experimental groups were defined: (1) Dbh-cKO ($Cre^{+}Flox^{+}TAM^{+}$); (2) Cre^{+} vehicle control ($Cre^{+}Flox^{+}TAM^{-}$); (3) floxed TAM^{+} control ($Cre^{-}Flox^{+}TAM^{+}$); and (4) floxed baseline control ($Cre^{-}Flox^{+}TAM^{-}$). Six- to nine-week-old mice received TAM administration via oral gavage (100 mg/kg) or intraperitoneal (50 mg/kg or 35 mg/kg) for five consecutive days. Mice were monitored using echocardiography under general anaesthesia and permitted one-week recovery. Mice treated with 100 mg/kg experienced complete lethality and were excluded from downstream analysis. Electrophysiological experiments were performed during sixteen- to eighteen-weeks of age. Mice were intraperitoneally anaesthetised with 0.3 mL of 1.2% 2,2,2-tribromoethanol and 0.3 mL of 2500 U/mL heparin to prevent clot formation. After five minutes, mice were humanely sacrificed by cervical dislocation in accordance with the United Kingdom Animals (Scientific Procedures) Act 1986. Hearts were excised and retrogradely perfused at physiological temperature via Langendorff apparatus with oxygenated Krebs-Henseleit buffer. Two pacing protocols were employed: (1) S1S1—twenty consecutive pulses at 100 ms cycle length with 5 ms decrements until 2:1 AV conduction block (Wenckebach point, WBP-AV); and (2) S1S2—a train of eight S1 stimuli followed by a single premature S2 stimulus with progressively shortened S1S2 intervals to determine the AV nodal effective refractory period (AVNERP).

Results

Statistical analyses were conducted in GraphPad Prism v10.5.0 using Shapiro-Wilk tests for distributional normality and Kruskal-Wallis tests for non-parametric comparisons. Data presented as median ± interquartile range. Median RR-intervals were broadly comparable: Dbh-cKO (n = 3) 213.4 ± 34.0 ms; $Cre^{+}Flox^{+}TAM^{-}$ (n = 2) 206.0 ± 16.0 ms; $Cre^{-}Flox^{+}TAM^{+}$ (n = 3) 179.5 ± 45.5 ms; and $Cre^{-}Flox^{+}TAM^{-}$ (n = 2) 243.3 ± 66.8 ms (P = 0.5783). AVNERP demonstrated no significant differences: Dbh-

cKO (n = 3) 80.0 ± 10.5 ms; $Cre^{+}Flox^{+}TAM^{-}$ (n = 1); $Cre^{-}Flox^{+}TAM^{+}$ (n = 3) 86.0 ± 11.5 ms; $Cre^{-}Flox^{+}TAM^{-}$ (n = 2) 79.0 ± 7.0 ms (P = 0.8163). WBP-AV were comparable: Dbh-cKO (n = 2) 100.0 ± 5.0 ms; $Cre^{-}Flox^{+}TAM^{+}$ (n = 3) 100.0 ± 0.0 ms; and $Cre^{-}Flox^{+}TAM^{-}$ (n = 2) 97.5 ± 2.5 ms (P = 0.4286). One Dbh-cKO mouse exhibited non-sustained ventricular tachycardia following S1S2 pacing at a 77 ms coupling interval, suggestive of provocation-induced conduction instability.

Conclusions

These preliminary findings provide the first functional assessment of AV nodal conduction following adult-onset cardiomyocyte-specific deletion of Dbh. While no statistically significant intergroup differences in basal conduction metrics were observed, the emergence of provocation-induced arrhythmia in a Dbh-cKO heart suggests a potential role for Dbh-CMs in preserving AV nodal function.

C27

Effects of neuronal remodelling in heart failure on regional ventricular electrophysiology in the rabbit heart.

Reshma Chauhan[1], Emily Allen[1], John Mitcheson[1], Richard Clayton[2], G. Andre Ng[1]

[1]University of Leicester, United Kingdom, [2]University of Sheffield, United Kingdom

Introduction: Sudden cardiac death remains a significant unresolved clinical problem resulting in more than 100,000 deaths per year in the UK. The majority of these deaths are due to lethal heart rhythm disturbances such as ventricular fibrillation however, the underlying mechanisms are poorly understood and there is no effective preventative treatments. Heart failure (HF) data support that the disturbance in autonomic control is a strong prognostic marker of sudden death due to ventricular arrhythmias; with sympathetic nerve activity reported to be heightened in HF. Electrical heterogeneity of the heart is also well recognised and is attributed to regional differences in sympathetic nerve innervations, ion channel distribution and action potential duration (APD); all of which become remodelled in HF. However, detailed studies into sympathetic innervations in HF and the effects on regional cardiac electrophysiology are lacking. This study aims to investigate the spatial cardiac heterogeneities in HF and the regional effects of sympathetic nerve stimulation, both across the ventricular surface and between myocardial layers, using optical mapping and voltage sensitive dyes of different wavelengths.

Methods: Adult male New Zealand White rabbits (3-3.5kg) were randomized to have coronary ligation surgeries (MI group, n=5) or sham procedures (Sham group, n=5) following premedication (Sedator 0.2mg/kg, Ketamine 10mg/kg and Torbugesic 0.05mg/kg). Anaesthesia was maintained using isoflurane and then an 8 week post-operative period was observed. Rabbits were then premedicated as before, prepared for heart isolation and administered terminal anaesthesia (Pentobarbitone sodium, 60mg i.v.). Using the isolated innervated rabbit heart preparation, optical action potentials were obtained with voltage sensitive dyes di-4-ANEPPS and di-4-ANBDQBS over the anterior left ventricle using a Hamamatsu 16×16 element photodiode array. Pacing protocols were performed via a catheter in the right ventricle, in the presence and absence of sympathetic nerve stimulation (SNS) via the spinal cord. Action potential duration (APD) and restitution (APDR) data were recorded. Data are mean±SEM; compared using ANOVA.

Results: MI hearts had a greater change in APD with SNS across the anterior left ventricle when compared to Shams; particularly in the mid-anterior wall (MI -5.02±2.1ms, Sham -1.25ms±0.2; $p<0.05$) and mid-apex (MI -5.30±2.2ms, Sham -1.24±0.2ms; $p<0.05$) regions when using di-4-ANEPPS. A similar response was seen with the deeper penetrating dye, di-4ANBDQBS, with the basal-freewall corner region showing the greatest change in APD in MI hearts (MI -5.56±1.3ms, Sham -3.17±0.6ms; $p<0.05$). These regions correlated with greater changes in in the slope of the APDR curve (di-4ANEPPS: MI mid-anterior wall 0.24±0.04, MI mid-apex 0.10±0.02; Sham mid-anterior wall 0.03±0.03, Sham mid-apex 0.06±0.03 (ns), and di-4-ANBDQBS: MI base-freewall corner 0.18±0.2, Sham base-freewall corner 0.07±0.06 (ns)).

Conclusion: MI groups showed greater, regionally specific changes in cardiac electrophysiology in the presence of SNS as a result of regionally specific heterogenous remodelling. These data detail spatial

and transmural heterogeneities in electrophysiology which could be key mechanisms underlying the increased susceptibility of arrhythmia in HF. Our findings underscore the importance of regional sympathetic modulation in shaping electrophysiological responses post-MI and suggest that targeted modulation of sympathetic inputs may offer novel therapeutic potential for reducing arrhythmic risk in HF patients.

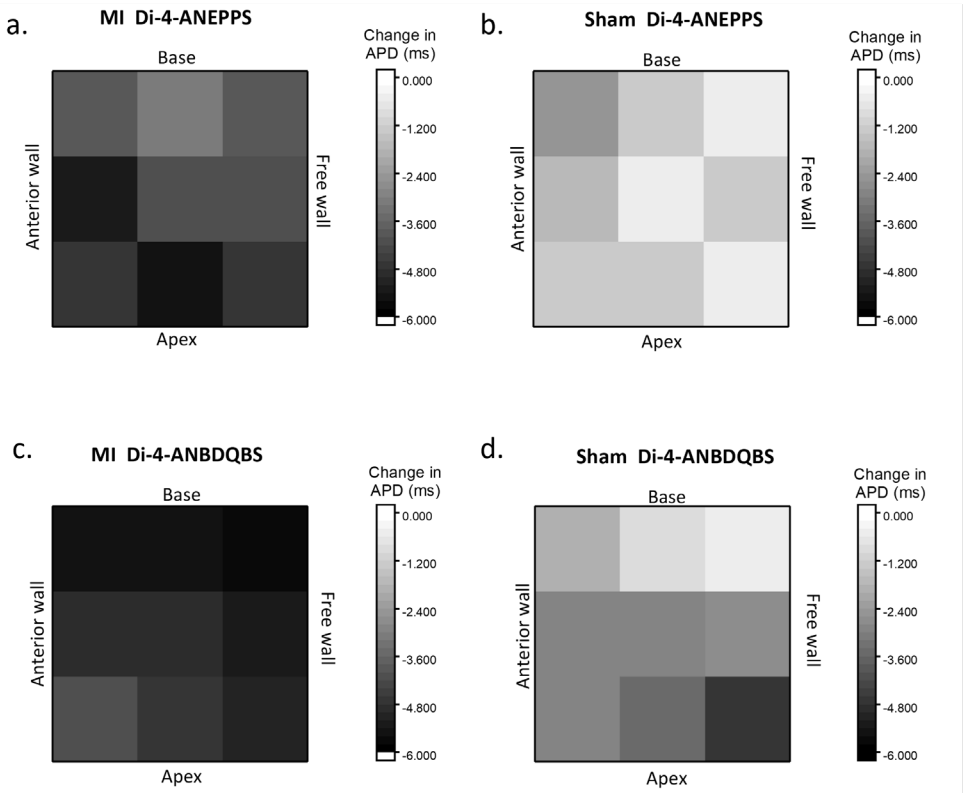

Figure 1. Change in action potential duration in the presence of sympathetic nerve stimulation across the anterior left ventricle. *9-grid plots showing changes from baseline action potential duration (APD) to APD in the presence of sympathetic nerve stimulation, across the anterior left ventricle, measured using optical mapping. Changes in APD with the shorter wavelength dye di-4-ANEPPS in the myocardial infraction (MI) model of heart failure (a) and sham model (b). Changes in APD with the longer wavelength dye di-4-ANBDQBS in the myocardial infraction (MI) model of heart failure (c) and sham model (d). Data are mean values averaged from a 256 pixel grid (16x16); n=5 for MI group, n=5 for Sham group.*

Cross-Talk of Cells in the Heart 2025: Novel Mechanisms of Disease and Arrhythmias
University of Birmingham, UK | 03 – 04 September 2025

C28

Ventricular inward sodium and outward potassium currents were inhibited by extracellular alpha-synuclein aggregates in situ

Bonn Lee[1], Charlotte Edling[1], Kamalan Jeevaratnam[1]

[1]School of Veterinary Medicine, University of Surrey, United Kingdom

Background: Alpha-synuclein, the major constituent of Lewy bodies (LB), is associated with neurodegeneration in Parkinson's disease (PD). Recent studies have reported an increasing recognition of cardiac complaints in PD patients and the cardiac pathologies associated with alpha-synuclein (Javanshiri et al. 2023; Lee et al. 2023). Particularly, the development of arrhythmias in PD patients may indicate potential electrophysiological alterations in the heart. Alpha-synuclein aggregates have been known to have disruptive effects on cell electrophysiology (Schmidt et al. 2012; Ferreira et al. 2017). However, their effect on the neurocardiac system has remained unknown.

Objectives: We investigated whether the exogenous application of alpha-synuclein aggregates affects the ventricular myocardium and stellate ganglia, potentially disrupting the electrophysiological integrity of the neurocardiac system.

Methods: We measured the in situ sodium and potassium currents from murine ventricular myocardium and stellate ganglia using the loose patch clamp technique (Lee et al. 2025). Male mice (C57BL/6) tissues were collected (n = 6 per group), followed by decapitation, conforming to the institutional guidelines (AWERB review reference: NASPA-1819-25 Amend 1) and the Animal (Scientific Procedures) Act. The tissues were exposed to bioactive extracellular alpha-synuclein aggregates, and currents were measured under three different conditions: baseline, alpha-synuclein treatment, and wash out (n = 18 patches per group, from six independent experiments).

Results: The result showed that alpha-synuclein aggregates altered the maximum sodium current (INa(Max)) (ANOVA, $p < 0.008$) and affected its gating properties for channel activation (ANOVA $F_{2,54} = 6.408$, $p = 0.003$) and inactivation ($F_{2, 67} = 6.32$, $p = 0.003$). The alpha-synuclein aggregates also reduced the maximum outward potassium current (IK(Max)) during channel activation ($F_{2, 77} = 6.02$, $p = 0.002$). However, the alpha-synuclein aggregates did not affect the ionic currents in the stellate ganglia.

Conclusion: Our results demonstrated that alpha-synuclein aggregates can inhibit ventricular ionic currents but do not affect the stellate ganglia, suggesting differential sensitivity between the myocardium and the stellate ganglia and indicating cardiac-specific toxicity of alpha-synuclein on cardiac electrophysiology in PD.

C29

Of men, not mice: strategic implementation of human hearts donated for research in the UK for the mechanistic interrogation of living myocardial slices

Sam Reitemeier[1], Danika Hayman[1], Parisa Keshtkar[1], Fani Koutentaki[1], Lorenza Koppers[1], Fatemeh Kermani[1], Cesare Terracciano[1]

[1]Imperial College London, United Kingdom

Mechanistic discoveries mostly rely on animal research or bioengineered human models. However, these platforms often fail to recapitulate human physiology and disease. Here we report a novel approach using adult human hearts, available from the UK NHS Blood and Transplant service, explanted exclusively for research and employed to prepare living myocardial slices (LMSs).

LMSs are ultrathin (300µm) sections of living cardiac tissue that can be prepared using a vibrating microtome from many species, including humans; LMSs maintain the native structure of the heart and can be kept in culture for weeks/months under physiological electro-mechanical conditions. We assessed whether preparing LMSs from donor human hearts is a viable and practical alternative to other research platforms.

From July 2024 to May 2025, we received 176 donor human heart offers. We accepted and used 31 hearts (15 of which donated after circulatory death, 16 donated after brain death), an almost ten-fold increase compared with previous years. The donors were 61 +/- 15.9 years of age (Mean +/- SD). We only accepted hearts from donors without cardiovascular disease or current infections and were within 6hrs transport time (transported in saline solution at 4°C). LMSs were prepared as described by our group previously (Camelliti et al., 2011; Pitoulis et al., 2020; van der Geest et al., 2025; Watson et al., 2019, 2017).

We could prepare 30-50 LMSs from a $1cm^3$ LV transmural biopsy. LMSs were viable and robust: (force transient amplitude at 2.2µm sarcomere length: 8.8 +/- 7.2mN/mm^2; passive force: 9.4 +/- 6.6mN/mm^2 (n=39)).

We also tested if it is possible to delay tissue utilisation, to facilitate high throughput, help with the arrival of tissue out-of-hours, and share it with other centres. There was no statistical difference in both force transient amplitude and passive force between fresh LMS and LMS from biopsies stored in cardioplegia for 5 hours at 4°C (active force fresh: 7.8 +/- 4.8mN/mm^2; post-cardioplegia: 26.4+/-24mN/mm^2; paired t-test: p=0.272; passive force fresh: 6.1+/-1.34mN/mm^2; cardioplegia: 13.5+/-5.4mN/mm^2; p=0.132, n=3 hearts from 8 fresh and 11 post-cardioplegia LMSs).

Adult donor heart tissue is a viable source of LMSs and can lead to valuable research in mechanisms of disease and treatment, as a valid alternative to animal research or bioengineered models.

Cross-Talk of Cells in the Heart 2025: Novel Mechanisms of Disease and Arrhythmias
University of Birmingham, UK | 03 – 04 September 2025

C30

RUNX1 as a therapeutic target for arrhythmia post-MI

Alexander Johnston[1], Adriana Gamboa Delgado[1], Hannah Fulton[1], Rosie Tudor[1], Stuart Nicklin[1], Ewan Cameron[1], Chris Loughrey[1], Rachel Myles[1], Eilidh MacDonald[1]

[1]University of Glasgow, United Kingdom

Following myocardial infarction (MI), a heterogenous transition zone between the scar and healthy myocardium develops. The region of myocardium bordering an infarct (border zone, BZ) undergoes many transcriptional changes, some of which may drive adverse remodelling. RUNX1, a master-regulator transcription factor intensively studied in the cancer and blood research fields, is increased in BZ cardiomyocytes at 1-day post-MI. Previously, we have shown that cardiomyocyte-specific Runx1 deficient ($Runx1^{\Delta/\Delta}$) mice demonstrate remarkably preserved systolic function at 1-day post-MI via increased cardiac sarcoplasmic reticulum (SR) calcium uptake highlighting RUNX1 as a novel modulator of contractile function (McCarroll et al. 2018). We then interrogated regional differences in Ca^{2+}-handling at 1-day post-MI by performing Ca^{2+} imaging in BZ and remote zone (RZ) cardiomyocytes from $Runx1^{\Delta/\Delta}$ and flox control ($Runx1^{fl/fl}$) mice. Overall, we found that BZ cardiomyocytes from $Runx1^{fl/fl}$ mice displayed impaired calcium handling compared to RZ cardiomyocytes, whereas there were no regional differences in $Runx1^{\Delta/\Delta}$ mice (Martin et al. 2023).

Ventricular arrhythmias, which can be driven by regional electrophysiological heterogeneity and impaired calcium handling, are a major complication of MI, with the BZ region being the most vulnerable site for arrhythmogenesis (Qin et al. 1996; Smaill et al. 2013). As such, we hypothesised that RUNX1 could play a crucial mechanistic role in the arrhythmogenicity of the ventricle post-MI.

To study this, we performed surface ECG studies in $Runx1^{\Delta/\Delta}$ and $Runx1^{fl/fl}$ mice in the early days post-MI (specifically days 1, 7, and 14) when the ventricle is most susceptable to arrhythmia to elucidate the role of RUNX1 on electrophysiology and arrhythmogenesis. ECG morphology was consistent between $Runx1^{\Delta/\Delta}$ and $Runx1^{fl/fl}$ mice pre-MI. However, we found that although QT interval was prolonged post-MI in both groups reflecting increased electrical heterogeneity, QT interval was shorter in $Runx1^{\Delta/\Delta}$ compared to $Runx1^{fl/fl}$ mice. We then used an intraperitoneal injection containing isoproterenol and caffeine was used to stress the cardiovascular system to evaluate the propensity for arrhythmia. We found that $Runx1^{\Delta/\Delta}$ had significantly fewer premature ventricular excitations compared to $Runx1^{fl/fl}$ mice.

Further, in ventricular cardiomyocytes isolated from C57BL/6 mice and incubated with Runx1 small molecule inhibitor Ro5-3335 or with vehicle control DMSO, we utilised a burst pacing protocol followed by a two-minute period of rest and measured spontaneous calcium events as a measure of arrhythmogenicity. We found that cells treated with Ro5-335 had significantly fewer spontaneous events in the rest period compared cells incubated in DMSO.

These findings indicate that RUNX1 contributes to arrhythmogenic calcium heterogeneity in the BZ post-MI, and its inhibition may mitigate arrhythmia risk by preserving calcium handling and reducing electrophysiological heterogeneity.

C31

Developing p21-activated kinase 1 (PAK1) activators to treat hypertrophic cardiomyopathy (HCM)

Yu He[1], James. S. H. Bae[1], Xin Wang[2], Ying-Jie Wang[1], Hugh Watkins[1], Ming Lei[1]

[1]University of Oxford, United Kingdom, [2]The University of Manchester, United Kingdom

Research rationale: Despite significant progress in comprehending the genetic and metabolic underpinnings of cardiomyocyte dysfunction, there is still a pressing need for targeted treatments to address hypertrophy and progressive remodelling (e.g., fibrosis), seen in HCM [1]. PAK1, a regulator of ion channels and myofilaments in cardiomyocytes, has shown promise in curbing pathological hypertrophy [2]. Our hypothesis centres on the potential therapeutic benefits of pharmacologically activating PAK1 in managing hypertrophy and adverse remodelling in HCM.

Methods: Molecular docking and high-throughput kinase assays using RapidFire-mass spectrometry were employed for virtual and physical screening to develop PAK1 activators. The effect of these activators on cellular hypertrophy was assessed using hypertrophic neonatal rat cardiomyocytes (n=200-300) induced by isoprenaline (ISO, 40 μM). Subsequently, the small molecule PAK1 activator JB2020A was evaluated in a well-characterized transgenic mouse model expressing the hypertrophic cardiomyopathy-causing mutation Actc1^{E99K}, known for its rapid disease progression [3]. A six-week oral treatment regime (10 mg/kg/day of JB2020A, Vehicle, and WT, N=5 in each group) was initiated at 4 weeks of age. The therapeutic efficacy of these pharmacological interventions and the endpoints were assessed using echocardiography, histology including Sirius red staining and H&E staining, and biomarker assessment using western blot. Data were analysed as mean ± SEM, and statistical significance was calculated using one-way ANOVA with Tukey's posthoc test.

Results: We have identified potent and effective small molecule PAK1 activators that significantly increased PAK1 activity by 3 to 5-fold, with an EC50 range between 0.5 and 2.5 μM. Through the evaluation of PAK1 activators on cellular hypertrophy, JB2020A not only prevented ISO-induced hypertrophy but also reversed pre-existing cellular hypertrophy induced by ISO 24 hours earlier. Moreover, after 6 weeks of JB2020A treatment, we observed a significant reduction in cardiomyocyte hypertrophy and cardiac fibrosis, accompanied by preserved cardiac function in Actc1^{E99K} HCM mice compared to vehicle treatment. These cardio-protective effects were associated with increases in phosphorylated PAK1 observed after activator treatment. Furthermore, JB2020A treatment resulted in a reduction in pro-apoptotic CHOP expression and an upregulation of protective endoplasmic reticulum (ER) response molecules (such as ATF4 and Xbp1), suggesting an amelioration of ER stress in HCM.

Conclusions: Collectively, these findings underscore the therapeutic potential of small molecule PAK1 activators as a novel approach for addressing hypertrophy and progressive remodelling in HCM.

Cross-Talk of Cells in the Heart 2025: Novel Mechanisms of Disease and Arrhythmias
University of Birmingham, UK | 03 – 04 September 2025